Electrical Power and Energy Systems 148 (2023) 108951

Contents lists available at ScienceDirect

International Journal of Electrical Power and Energy Systems

journal homepage: www.elsevier.com/locate/ijepes

An ILP model for stochastic placement of μPMUs with limited voltage and current channels in a reconfigurable distribution network

Nasim Khanjani, Seyed Masoud Moghaddas-Tafreshi *

Department of Electrical Engineering, University of Guilan, Rasht, Iran

ARTICLE INFO

Keywords:
Stochastic μPMU placement
Channels limit
Reconfiguration
Integer linear programming (ILP)

ABSTRACT

Micro phasor measurement units (μPMUs) play a major role in the evolution of distribution networks toward the smart grids by providing precise and synchronized measurements. In this study, an integer linear programming (ILP) model for stochastic optimal μPMU placement (SOMPP) problem is formulated in order that the network would remain observable following a network reconfiguration. Furthermore, the current measurement channels are considered limited and it is also extended to voltage measurement channels, in order to be employed in cases that measurement channels are insufficient (e.g. three-phase networks). The uncertain quantities including the variability of load demands and the unreliability of lines are characterize by proper probability distribution functions (PDFs) instead of constant values, and employed in a Monte Carlo simulation (MCS) process. The most probable scenarios are obtained by a scenario reduction method, and the most probable topologies within each scenario are identified by multiple execution of reconfiguration for the reduced scenarios using the genetic algorithm (GA). Then the SOMPP model is solved for each reduced scenario using the concept of equivalent network that is also introduced in present work. A formulation for the deterministic form of the problem is also developed in order to compare the results of the SOMPP model with the deterministic one, by which the observability of all possible topologies is guaranteed with a limited number of channels. Furthermore, using the concept of voltage channels limit, the formulation of the SOMPP model is extended to include the unbalanced networks. The simulations are performed on 33-bus and 240-bus distribution networks. The numerical results revealed the relative superiority of the SOMPP model over the deterministic version and previous works in terms of decreasing the required number of μPMUs. Moreover, the effectiveness of the model in handling the random variables with unknown PDFs is also determined. The success of the reduced scenarios in representing the most general scenarios is also demonstrated by evaluating a large number of scenarios. The validation of the concept of equivalent network is also examined for multiple simulation cases.

1. Introduction

Real-time monitoring is a key element in transition of the traditional distribution networks toward the smart grids. The phasor measurement units (PMUs) are one of the latest types of measurement devices that are able to measure real-time phasors of voltage and current with high accuracy [1,2]. A PMU installed at a bus could measure the voltage phasor of its own bus and all the current phasors of the adjacent lines theoretically [1,3–13]. Accordingly, using the circuit laws, the voltage phasors of the buses connected to a PMU bus would be measured indirectly, so a PMU could make its own bus and ideally all its adjacent buses observable. However, the number of measurement channels of the PMUs are limited in practice and they could observe a number of their adjacent buses. Thanks to the capability of measuring both current and voltage by PMUs, the observability of the network could be provided by a limited number of them. The number and the locations of the PMUs could be determined through optimal PMU placement (OPP) problem in order to make the network observable with minimum cost or minimum number of PMUs [4–6]. As distribution networks become smarter and more complex, defining a fixed situation for the network would become more difficult. The integration of elements with uncertain nature, the probability of components' failure, and the dynamic topology are some of the issues that real distribution networks are getting involved with. Considering the aforementioned uncertainties, variabilities, and limits, in the OPP problem could make it more applicable for the real world problems.

There are plenty of studies in the literature on the issue of deploying PMUs in the transmission networks [1–5,8–21]. However, the number

* Corresponding author.
E-mail address: tafreshi@guilan.ac.ir (Seyed Masoud Moghaddas-Tafreshi).

https://doi.org/10.1016/j.ijepes.2023.108951
Received 20 May 2022; Received in revised form 13 November 2022; Accepted 3 January 2023
Available online 14 January 2023

Nomenclature

Parameters

N	Number of network buses.
S, S'	Initial and reduced number of MCS scenarios.
L	Number of μPMUs/PMUs channels.
T_0	Optimal topology of the network when no lines are failed.
p_s	Probability of scenario s.
c_i	Cost of installing PMU at bus i.
d_i, d_i^{3PH}	Degree and three-phase degree of bus i, respectively.
n_i^{TS}	Number of tie-switches connected to bus i.
G_{ij}, B_{ij}	Conductance and susceptance of the line connecting buses i and j, respectively.
PL_i, QL_i	Active and reactive power of loads at bus i, respectively.
λ_l	Hazard rate of line l.
$\mu_{pl_i}, \sigma^2_{pl_i}$	Mean value and variance of the active power of load at bus i, respectively.
$\mu_{ql_i}, \sigma^2_{ql_i}$	Mean value and variance of the reactive power of load at bus i, respectively.
r_i	Number of ways that a μPMU/PMU could be installed at bus i.
r_{sti}	Number of ways that a μPMU/PMU could be installed at bus i for tth topology of scenario s.
$r_{si}^{EQ}, r_{sih}^{EQ}$	Number of ways that a μPMU/PMU could be installed in equivalent network of scenario s at bus i and at phase h of bus i, respectively.
b_j	Desired observability value of bus j.
b_j^R, b_j^{RCL}	Desired observability value of bus j for OPP/OMPP considering reconfiguration and deterministic problem, respectively.
b_{sj}, b_{stj}	Desired observability value of bus j for scenario s and for tth topology of scenario s.
b_{sjh}^{EQ}	Desired observability value in equivalent network for scenario s at phase h of bus j.
a_{ji}	Observability coefficient of bus i relative to bus j.
$a_{ji}^R, a_{ji}^{meshed}$	Observability coefficient of bus i relative to bus j for OPP/OMPP considering reconfiguration and for meshed network, respectively.
$a_{jik}^{CL}, a_{jik}^{RCL}$	Observability coefficient of bus i relative to bus j for the kth way of installing μPMU/PMU at bus i for OPP/OMPP considering channel limit and deterministic problem, respectively.
a_{stjik}	Observability coefficient of bus i relative to bus j for the kth way of installing μPMU/PMU at bus i for tth topology of scenario s.
$a_{sjik}^{EQ}, a_{sjgihk}^{EQ}$	Observability coefficient of bus i relative to bus j and phase h of bus i relative to phase g of bus j, respectively, for the kth way of installing a μPMU/PMU at bus i in equivalent network for scenario s.

Functions

pl_i, ql_i	PDFs of active and reactive power of loads of bus i, respectively.
f_l	PDF of the failure of line l.

Indices

s, t, τ	Indices of scenarios, topologies, and time, respectively.
i, j	Bus indices.
k	Index of the ways that a μPMU/PMU with limited channels could be installed at a bus.
g, h	Phases indices.
l	Index of lines.

Sets

Γ_s	Set of topologies within scenario s.
Δ	Set of lines that are not equipped with a tie switch.
Ω	Set of buses that are connected to the switches that may change the state or lines that may fail in the equivalent network.
$\Lambda_i, \Lambda_{ik}^L$	Sets of adjacent buses of bus i and the kth L-subset of Λ_i, respectively.
$\Lambda_i^{3PH}, \Lambda_{ik}^{L3PH}$	Sets of adjacent bus phases of bus i and the kth L-subset of Λ_i^{3PH}, respectively.

Variables

v_i, δ_i	Voltage magnitude and phase angle of bus i, respectively.
x_{ij}	Binary status of the line connecting buses i and j.
pg_i, qg_i	Active and reactive power generation at bus i, respectively.
x_i	Binary decision variable of installing a μPMU/PMU at bus i.
$x_{ik}^{CL}, x_{ik}^{RCL}$	Binary decision variable of the kth way of installing a μPMU/PMU at bus i for OPP/OMPP considering channel limit and deterministic problem, respectively.
x_{stik}	Binary decision variable of the kth way of installing a μPMU/PMU at bus i for tth topology of scenario s.
$x_{sik}^{EQ}, x_{sihk}^{EQ}$	Binary decision variable of the kth way of installing a μPMU/PMU in equivalent network for scenario s at bus i and at phase h of bus i, respectively.
o_j	Obtained observability for bus j.
o_{sj}, o_{sjg}	Obtained observability for bus j and for phase g of bus j, respectively, for scenario s.
o_{stj}	Obtained observability for tth topology of scenario s for bus j.

of research works on the topic in the area of distribution networks has also been increasing recently [6,7,22–30]. With emerging the micro phasor measurement units (μPMUs) that are less expensive and more accurate than traditional PMUs, deploying them in the distribution networks is becoming more sensible [7,29], especially for short distribution lines that the difference between the voltage magnitude and the phase angle at the beginning and the end of the lines is not significant [26,27]. Therefore, by upgrading the distribution networks toward a smarter version, the importance of fast and accurate data collection is becoming more plausible and accordingly, it justifies the increased research in the areas of deploying μPMUs and the challenges ahead in the distribution networks.

Even though PMUs and μPMUs are actually doing the same thing, i.e. providing accurate and real-time measurement data for monitoring the network, μPMUs have some specific features and requirements. The total cost of μPMUs depends on the costs of the main unit (which consists of electronic components), the potential transformer (PT), the current transformers (CTs), and transmitting data to the global central processing system [30]. In transmission networks, CTs and PTs are expensive in high voltage, while in distribution networks, medium and low-voltage transformers are not expensive [30]. Accordingly, the lower price of CTs and PTs could notably diminish the total cost of μPMUs. The sampling rate of the μPMUs is 256–512 Hz that caused the μPMUs to be significantly more accurate than PMUs (± 0.01 degrees), while the sampling rate of the PMUs is between 30 Hz to 60 Hz and the accuracy of the PMUs is ± 1 degrees. [30]. Since the μPMUs are employed for the real-time applications, the collected data by the μPMUs should be transmitted entirely and fast. There are two factors that are important in transmitting data; the channel capacity that is the maximum rate of data that could be transmitted through the communication channel of a μPMU, and the latency that is the length of time that it takes between creation the data and receiving it at the receiving unit. In real-time applications, low-latency channels are required. Among different communication channels, fiber optics and 4G and 5G communication networks are leading [31]. It is worth mentioning that, to the best of the authors' knowledge, the mathematical modeling of the PMUs and μPMUs placement problems are the same. Accordingly, the word PMU is used frequently throughout the present paper in order to discuss about the common features and models for both PMUs and μPMU, while the word μPMU is only used for the proposed model and also for describing the particular features of the μPMUs.

Some features of the distribution networks, such as variability of topology, make the OPP problem of the distribution networks different from its counterpart in the transmission networks. The observability of the network is affected by the topology variations. Therefore, the network would be exposed to unobservability due to reconfiguration [7, 24]. The unobservability makes the state estimation of the network impossible. Whereas the problem of losing observability during the reconfiguration is addressed in [32] by appending the observability constraint into the reconfiguration problem formulation, the problem would not be completely resolved because the observability would be preserved in exchange for deteriorating the reconfiguration objective function, i.e. minimizing active power loss. Therefore, a number of studies had incorporated the effect of topological changes in the OPP problem [6,7,22–25,28,29]. Most of the methods in the published works ensure the observability of the network for all or a number of possible topologies. Among the methods investigated in the literature, the authors of [6] had developed an OPP model that guarantees the observability of the network for every possible topology. The method of [6] would completely solve the problem of losing observability due to reconfiguration, but the number of PMUs would be increased as a result of including all possible topologies in the model, while there are a lot of topologies that would not be functioning because of unsatisfying the operational requirements of the network. Similar to [6], all feasible topologies are included in the placement scheme proposed in [28]. The placement solution in [28] should satisfy the observability constraint for all feasible topologies, while the method of [6] leads to a solution that provides observability for all topologies. There are a number of studies, in which maintaining the observability for a number of topologies is investigated. In [7] the reconfiguration is done for several load levels throughout a year, the OPP problem is solved for every obtained topology from reconfiguration, and the union of the solutions for all obtained topologies is suggested to be the ultimate solution. Similar to [7], the reconfiguration is performed for different hours of a typical day in a distribution network with intermittent photovoltaics and wind turbines in [22,23] and the OPP problem is solved for each obtained topology. By the approaches of [7,22,23], only the effect of load levels on the reconfiguration is addressed, whereas the reconfiguration is influenced by different variables such as faults. The number of PMUs obtained in [7,22,23] are also non-optimal, since the multiple topologies are not considered once in an aggregated OPP model, but the union of the solutions derived from solving the OPP model for a number of times is considered as the final solution. In [24], an approach proposed by which every tie switch must be equipped with a PMU at one of its connected buses to ensure the observability when they are operated. The method guarantees the observability of the buses that are connected to the tie switches, while the observability of other buses might become in danger due to opening the sectionalizing switches. In [25] a few pre-defined topologies are considered and attempted to find the locations of μPMUs to maximize the sum of observability of buses along with minimizing the number of μPMUs. As is claimed in [25], the method helps the network be partially observable in abnormal condition and full observability of the pre-defined topologies would not be ensured. The possibility of islanding is incorporated in the OMPP model of [29] so that all switches in the network are assumed to be opened, to accommodate all possible network reconfigurations and islanding. Eventhough the method of [29] considered the worst-case scenario, but the possibility of line failure is ignored that could lead to unobservability.

The number of PMU channels indicate the maximum number of current and voltage phasors that could be measured simultaneously by a PMU. Considering unlimited number of channels leads to an unrealistic and optimistic perspective. The more the number of channels become, the fewer PMUs will be needed to make the network observable [3,8]. While, the degrees of buses in the distribution network graph are less than the ones in the transmission network, utilizing the PMUs with great number of channels seems to be unnecessary in distribution networks. On the other hand, the channel capacity of μPMUs, that are designed for the distribution networks, are also limited [27]. Therefore, regarding the channels limit in the OPP problem, especially in the area of distribution networks, is unavoidable. It is also claimed in [27] that the total installing cost of a typical commercial μPMU with an extra channel would be increased by 6.5–20% while this additional cost will raise to 90–500% of the unit cost in low-cost μPMUs. Actually, the μPMUs with large number of channels need more CTs and PTs [27], that it could increase the total installing cost. Therefore, considering the channel capacity limit results in cost management in practice. The channels limit is taken into account in most of the studies carried out in the area of PMUs/μPMUs placement [3,4,8,11,19–21,25,27,28,30]. In most of the previously mentioned studies, the number of channels are considered identical for all the PMUs intended to be located in the network, but in [19], a nonhomogeneous mix of channel capacities is examined in order to minimize the costs and the waste of channels and being more practical. Nonhomogeneous number of channels, that is called hybrid current channels is also regarded in [27] to minimize the total cost and any unnecessary measurements. According to these facts, the limited number of channels are considered in present work. Furthermore, in all the aforementioned works, it is assumed that a PMU would always measure the voltage phasor of its bus, which means the PMU would always make its own bus observable, and the channel capacity limit is only for the current measurements. In some cases that multiple phases of a bus should be observed by a single-phase PMU, it is impossible for the PMU to make its bus completely observable. Accordingly, the channel capacity restrictions could be extended to include the voltage phasor measurements as well.

In most of the works in the literature, the determinant factors in the OPP model are considered deterministic. But actually, there are some degrees of uncertainty in the network that it would be more realistic to capture them. There are a number of studies in which the uncertainties of the power network are included in the OPP model. Most of these studies have focused on the uncertainty concerned with the field of network reliability. One of the earliest works regarding the issue is [14]. In aforementioned paper, the probability of the observability of buses is introduced and properly formulated by the indices of the availability of components. The average of the probabilities of bus observability, called APO, is used as an objective to maximize the observability of buses along with minimizing the number of required PMUs. There are some other works that used a similar approach to build a probabilistic framework for the OPP such as [9,15]. The authors of [17] used a same approach as [14] along with the effect of zero injection buses (ZIBs) and limited observability propagation which are reflected in the formulation. In [16], the probabilities of PMUs/lines outages are considered in an multi-objective optimization model aiming to minimize the cost of PMUs and the number of unobservable buses affected by PMUs/lines outage contingencies. Another multi-objective and bi-level probabilistic reliability-based model is proposed in [10] to minimize simultaneously the number and the unavailability of PMUs and the probabilities of lines outages. In [11] a set of scenarios are generated by Monte Carlo simulation (MCS) using the availability of the network components. In each scenario, some equipments would be out of service. The most probable scenarios are identified out of generated scenarios for simultaneous placement of PMUs and flow measurements. In [21], the probability of the network being fully observable is maximized as well as the number of PMUs being minimized. The probability distribution function (PDF) of uncertain variables are not included in any of the aforementioned studies, and indeed, the value of probabilities assumed to be fixed. But the uncertain variables are described by PDFs in practice. In [18], the probabilities of the failure of lines are characterized by exponential function. The probability of unobservability of each bus is formulated as a function of failure probability of lines and the probability of observability of the whole network is derived from them. The Markov chain is used to calculate the probabilities of cascading outage paths of network lines, and the consequences of the severity of cascading outages are quantified by proper indices and utilized in an optimization problem to minimize the risk of losing observability and the number of PMUs. Even though the failure probabilities are not considered fixed in [18], but the formulation of failure PDF indicates that the failure of lines are only associated with their overloadings, while the reliability of lines are dependant to time as well. Furthermore, in all of the studies reviewed, other sources of uncertainty like loads are ignored. The uncertainty associated with loads and lines failures are considered simultaneously in the present work by proper PDFs and utilized in a probabilistic framework to determine the most probable topologies and the observability of the network for these topologies would be guaranteed by a μPMU placement approach.

Generally, there are two approaches for solving the OPP problem, mathematical programming and metaheuristic methods. In the mathematical programming models, the precise definition of the constraints is very important in achieving the solution [3,8]. They also result in a single solution, while there might be multiple solutions with the same number of PMUs [8]. Linear programming (LP) is widely used among the mathematical programming subfields for modeling the OPP problem [3,4,6,7,11,16,19–21,24–29]. By metaheuristic algorithms, multiple solutions could be obtained, but the long execution time of simulation for the large-scale models and the possibility of trapping in local optimum are the disadvantages of these methods [10]. A number of metaheuristic methods are employed in the literature, such as binary particle swarm optimization (BPSO) [1], genetic algorithm (GA) [2,13], constriction factor based particle swarm optimization (CF-PSO) [8], and cuckoo search algorithm (CSA) [15]. A different method is introduced in [5] in which the observability equations are defined by nonlinear polynomial equations and the model is solved using Groebner bases. In addition to aforementioned method, in [22,23] Greedy algorithm heuristic method is employed to provide the good quality approximation of the solutions instead of metaheuristics wherewith the global solution is not ensured. Nonlinear OPP models are developed in some studies whereas the difficulties in achieving the global optimal solution are associated with such models. Different approaches are employed for solving nonlinear models. In [14], the OPP problem is first formulated as a mixed-integer nonlinear programming (MINLP) model and then transformed to a mixed-integer programming (MIP) model by a linearization approach and solved by CPLEX solver. The same approach is adopted in [17], and the MINLP model is approximated by a linear approximation method. The similar problem to [14] was also expanded in [9,15], and the nonlinear problem is solved using BONMIN solver and CSA, respectively. In [18], the problem is formulated as a MINLP model and the optimal solution is found by Branch and Bound method in the Knitro optimization engine. In [12] a MINLP formulation is proposed and solved by a two-phase branch-and-bound algorithm.

Zero injection buses (ZIBs), i.e. buses with no loads and generations, are generally attended in the OPP problems, especially in the area of transmission network, because of their features which improves the observability of the network by fewer number of PMUs. But, according to [15], ZIBs are a virtual concept that would not be practically possible, because the buses with neither generations nor loads still have some internal consumption for posts and equipments, so, they are not actual ZIBs. Furthermore, even if an actual ZIB does exist, it might become non-ZIB due to the expansion of the network in the future. Especially in the distribution networks that loads are dispersed roughly at whole buses across the feeders. Therefore, the ZIBs are ignored in the present work.

In present paper, an ILP model for the stochastic optimal μPMU placement (SOMPP) problem is developed to address the issue of losing observability due to reconfiguration. Using the stochastic model, the most probable topologies of the network are identified, instead of considering all of them, and attempts were made to provide the observability of topologies by appropriate placement of μPMUs, to decrease the required number of μPMUs. The uncertainty is reflected in the model by proper PDFs rather than a constant probability value. The restriction of measurement channels is not only applied on current channels, but restriction of the voltage measurement channel is also introduced that helps the formulation of the SOMPP be expanded to three-phase unbalanced networks; however, the main formulation of present work is devised to be solved for a single phase. The 33-bus benchmark distribution network and 240 bus distribution test network are used to implement the proposed model. The contributions of the paper are highlighted in the following:

1. The stochastic model, proposed in present study includes the uncertainty of loads as well as the unreliability of lines, to obtain a more realistic perspective. The PDFs of the lines failures are also employed instead of using a constant value for the availability of lines and they are used in a MCS process to generate scenarios.
2. The topologies that are more likely to be happened are identified with their probabilities, to cover the most common variations that might happen in the network topology as a result of the lines outages and changes in the load values.
3. The limitation of the number of channels of the μPMUs is not only applied for current measurements, but the voltage measurement limit is also introduced that helps the SOMPP model be generalizable to three-phase unbalanced networks. It means that the voltage measurement of the μPMUs buses would not be available all the time, but the voltage phasors are measured according to the preferences of the model.

The remaining parts of the paper are structured as follows: In Section 2, the formulation of the ILP model for the SOMPP problem considering the measurement channels restriction is evolved, in order to avoid unobservability following a network reconfiguration. Next, in Section 3, the test systems are introduced and the simulation inputs are given.

Then the numerical results are stated and discussed in the rest of the section. Finally in Section 4, the conclusion and the suggestions for the future works are given.

2. Problem formulation

In this section, the formulation of the proposed ILP model for the SOMPP problem is presented. By this approach, instead of all possible topologies, only the most probable ones are considered. The deterministic version of the problem in which all the possible topologies, even ones with low probability of being applied, are taken into account would also be brought in Appendix A to compare the results of the stochastic and the deterministic approaches.

2.1. The proposed SOMPP model

As mentioned in the introduction, the method introduced in [6] leads to the solution that includes all the possible topologies of the network. While there are a lot of topologies for a typical distribution network that are feasible from the topological point of view (leading to connected and radial network), but not optimal in terms of operational criteria. Therefore, the probability of deploying most of the feasible topologies is extremely low. Consequently, considering these less probable topologies in the SOMPP problem is not beneficial in practice.

On the other hand, the nature of power networks is associated with uncertainties. The uncertainties arise from the variability of the electrical quantities and the unreliability of the network elements. The variability of loads is an uncertainty source in the normal operational condition of the network. There are some other uncertainty sources like the generators that their output power is associated with solar or wind energy resources. In present work, under normal operational condition, only the uncertainty of the load points are taken into account. Another source of network uncertainty is unreliability of the network components such as lines, switches and etc. The reconfiguration is done under both normal and emergency conditions of a distribution network [33]. In normal condition, the reconfiguration is affected by the uncertainty of loads, while in an emergency, the reconfiguration is influenced by lines outages as well as loads variations. In the following subsections, finding the probability of occurrence of topologies under normal and emergency conditions is pursued. Then, these topologies and their probabilities are used in the SOMPP problem.

The time horizon of the proposed model is considered single year. Since the problem is related to the planning of the distribution network that is intrinsically long-term, the optimal solution of a single year may not be optimal for any other years. Especially in large-scale networks that due to high cost of μPMUs, installing the required number of μPMUs is not possible at once [15]. Therefore, the planning models are often multistage and designed to be solved for several years. There are plenty of multistage OPP/OMPP models in the literature [5,7,14,15]. In present work, the expansion of the network over the years is ignored. While, the model could be extended over a longer time horizon as a multistage problem.

As discussed so far, in order to form the proposed model, the PDFs of uncertain variables, i.e. loads and lines failures should be known or calculable. A large number of samples from PDFs, called scenarios, are generated and then the scenarios are reduced until a few representative scenarios are retained. In each reduced scenario, a number of lines are likely to be failed within the target year. Since the lines that expose to risk of failure in a scenario, have different time to failures (TTFs), they would not be failed at the same time, but one after another. At the moment $\tau = 0$ (the beginning of the target year), no lines are failed, so, the network would be in its initial optimal topology T_0. T_0 is the optimal topology of the network when no lines are failed and is obtained by reconfiguration.

Now, consider Fig. 1, in which the horizontal axis demonstrates the time of the target year (in hours). The topology T_0 is kept until $\tau = \tau_1$, when the first line failure is occurred. Then, the reconfiguration is done considering the line outage and the topology T_1 is determined and kept until the failed line is repaired. After repairing the failed line, the optimal topology would be T_0 again, because it is the optimal topology of the network when no lines are failed, and T_1 is the optimal topology when first line failure is imposed to the network. The topology T_0 is remained until $\tau = \tau_2$ when the next line failure is occurred. This procedure is kept up during the target year. Therefore, a number of topologies $\{T_0, T_1, \dots\}$, are obtained for each scenario. The repetitive topologies within each scenario are considered once. The topology T_0 is included in each scenario, because regardless to the scenario, T_0 would be the topology of the network if no line failure is occurred. If there was any other optimal topologies, like seasonal reconfiguration, they would be included in each scenario same as T_0.

In order to obtain the solution of the stochastic problem, the following optimization model must be solved for every scenario in order to find the set of possible solutions under each scenario condition. The network should remain observable for every topology of each scenario, so an optimization problem is devised in order to minimize the number of μPMUs, as well as considering all topologies within each scenario, as following,

$$\text{min:} \quad p_s \sum_{t \in \Gamma_s} \left(\sum_{i=1}^{N} \sum_{k=1}^{r_{sti}} x_{stik} \right), \tag{1}$$

$$\text{subject to :} \quad o_{stj} = \sum_{i=1}^{N} \sum_{k=1}^{r_{sti}} a_{stjik} \cdot x_{stik} \geq b_{stj}, \tag{2}$$

$$\forall s \in 1, 2, \dots, S', \quad t \in \Gamma_s, \quad j \in 1, 2, \dots, N.$$

In (1) and (2), r_{sti} and a_{stjik} could be calculated exactly by the method of obtaining r_i and a^{CL}_{jik} that will be introduced in Section 2.1.3. Each value of b_{stj} would be considered equal to one, in order to achieve the observability with minimum number of μPMUs.

According to (2), the set of solutions of each scenario provides the observability for all topologies within that scenario. However, the decision variables in each scenario are different for different topologies and could take different values, because the topologies are not dependent to each other. To address this problem, the concept of *equivalent network* would be introduced in this section. Accordingly, for each scenario, an equivalent network with unique topology would be constructed. The observability of the equivalent network of a scenario could provide the observability of all topologies within that scenario. The steps of building the equivalent network is described in the following using a small example network.

After obtaining optimal topologies within each scenario, the lines that might be failed and the switches that might become opened or closed would be known. Then, for each scenario, an equivalent network would be obtained. The equivalent network has some characteristics as follows:

1. The buses of the equivalent network are the same as the buses of the initial network.
2. The lines that never fail or the switches that are always closed within the scenario are shown in closed state in the equivalent network graph.
3. The switches that are always open within the scenario are shown as open branches in the equivalent network graph.
4. The lines that may fail and the switches that their states might be changed in different topologies, are also specified in the network graph by closed state. However, the observability of the buses connected to two ends of these lines/switches should not be provided through them, because by opening/failing these lines, the buses connected to the ends of these lines might become unobservable.

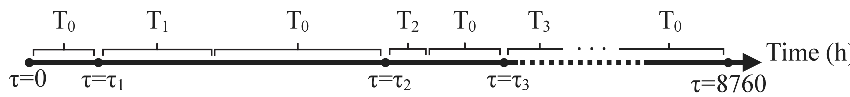

Fig. 1. Changes of the topology of the network during the target year.

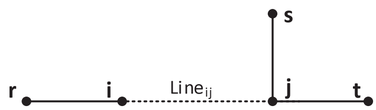

Fig. 2. An example of the equivalent network.

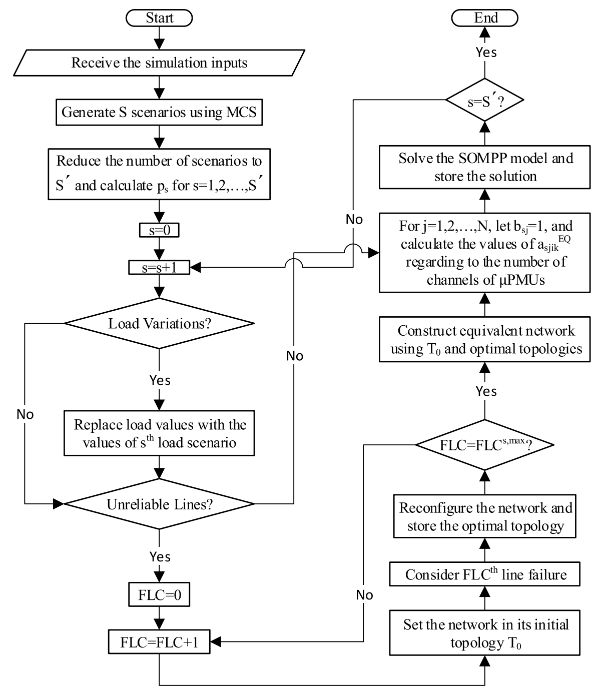

Fig. 3. The flowchart of the proposed SOMPP model.

In Fig. 2, an example of the equivalent network is given. The state of Line_{ij} would be changed within the scenario. The lines that are always closed within the scenario are illustrated by solid lines. In order to preserve the observability of the network when Line_{ij} is opened, the buses i or j should not be observed by the μPMUs of each other, because opening Line_{ij} would result in losing the observability of i or j. According to Fig. 2, the equation of the observability of buses i and j is obtained from

$$o_i = a_{ii}x_i + a_{ir}x_r + a_{ij}x_j, \tag{3}$$

$$o_j = a_{jj}x_j + a_{ji}x_i + a_{js}x_s + a_{jt}x_t. \tag{4}$$

In order to keep the observability of buses i and j when Line_{ij} becomes opened, the following inequalities should be satisfied;

$$a_{ii}x_i + a_{ir}x_r \geq 1, \tag{5}$$

$$a_{jj}x_j + a_{js}x_s + a_{jt}x_t \geq 1. \tag{6}$$

Accordingly, Eqs. (1) and (2) could be rewritten using the equivalent network concept as

$$\min: \quad p_s \sum_{i=1}^{N} \sum_{k=1}^{r_{si}^{EQ}} x_{sik}^{EQ}, \tag{7}$$

$$\text{subject to}: \quad o_{sj} = \sum_{i=1}^{N} \sum_{k=1}^{r_{si}^{EQ}} a_{sjik}^{EQ} \cdot x_{sik}^{EQ} \geq b_{sj}, \tag{8}$$

$$\forall j \in 1,2,\ldots,N, \quad s \in 1,2,\ldots,S'.$$

The superscript EQ above some of the parameters or variables in (7) and (8) indicates that these parameters or variables are dependent to the structure of the equivalent network, while those with no superscript are determined just same as (1) and (2). r_{si}^{EQ} and a_{sjik}^{EQ} are determined similar to the method of obtaining r_i and a_{jik}^{CL} in Section 2.1.3, but the set Ω that contains all the buses that are connected to the switches that are likely to change the state and the lines that are likely to be failed within the scenario, is defined and $\forall i \in 1,2,\ldots,N$, $k \in 1,2,\ldots,r_i$, $\Lambda_{ik}^{L} \bigcap \Omega$ would be deleted from Λ_{ik}^{L}, in order to prevent losing observability when aforementioned lines/switches are failed/operated.

The values of $b_{sj}, \forall j \in 1,2,\ldots,N$ is considered equal to one, in order to minimize the number of required μPMUs to make the network fully observable under circumstances of the problem.

The flowchart of the proposed algorithm is given in Fig. 3. According to the flowchart, after receiving the simulation inputs (that include initial network topology T_0, parameters, and loads and generators data, the number of channels of μPMUs, the initial and the reduced number of scenarios, the number of times that the reconfiguration program must be run, and, the genetic algorithm parameters), S scenarios are generated that include the scenarios of loads and the scenarios of the TTFs of lines. Then, the number of scenarios is reduced to S' and the probability of each scenario p_s is determined. Next, in each scenario s, if the uncertainty of loads is considered, the load values will be replaced by the sth scenario of loads. Then, if the unreliability of lines is also intended, for each line failure in scenario s (FLC is the failed line counter), first, the topology of the network is set to T_0, and then the state of the failed line is considered opened in T_0, and the reconfiguration is executed in order to find the optimal topology when the line is failed. Whenever the reconfiguration is done for all failed lines in scenario s ($\text{FLC} = \text{FLC}^{s,\max}$), the set of obtained optimal topologies are used to construct the equivalent network representation for scenario s. Afterwards, the parameters of the SOMPP model (a_{sjik}^{EQ} and b_{sj}) are determined and the SOMPP model is solved to obtain the optimal number and locations of μPMUs for scenario s. The procedure is repeated until obtaining the optimal solution for all scenarios.

In the following subsections, the required steps for building the SOMPP model are described in detail.

2.1.1. The basic OPP problem

The formulation of the OPP problem in order to make the network completely observable by PMUs that is commonly used in the literature [3–5,7,8,12,16,17,19,22–24,26,30] is as follows:

$$\min \quad \sum_{i=1}^{N} c_i x_i \tag{9}$$

$$\text{subject to}: \quad o_j = \sum_{i=1}^{N} a_{ji} x_i \geq b_j \quad , \quad \forall j \in 1,2,\ldots,N \tag{10}$$

The basic OPP problem is formulated as a linear programming (LP) model. The objective function (9) is aimed to minimize the total cost of installing PMUs while keeping the network observable with the restrictions imposed by the observability constraint (10). If $c_i = 1, \forall i \in$

$1, 2, \ldots, \mathrm{N}$, the OPP problem is converted to the problem of minimizing the number of PMUs. Since, in present work, the goal is to reduce the number of μPMUs, the cost coefficients are omitted from other cost function equations. In constraint (10), $\mathrm{a}_{ji} = 1$ if $i = j$ or if there is a line between buses i and j, otherwise, $\mathrm{a}_{ji} = 0$. If $\mathrm{o}_j \geq 1$, the network would be observable in its current topology. $\forall j \in 1, 2, \ldots, \mathrm{N}$, b_j is normally considered equal to one in order to minimize the required number of PMUs to make the network observable.

There are two different methods for observability assessment in the literature, numerical and topological methods [1,3,8,21–23,25,26]. The Topological observability analysis is the most commonly employed method to reduce the computational difficulties associated with the numerical analysis. The observability constraint (10) is formatted as a numerical observability framework. It is worth mentioning that, evaluating the observability of the network by checking the observability of each bus is not the only way of observability assessment. There are some studies in the literature like [28], that investigated the observability of each line using a different formulation, in order to evaluate the observability of the whole network.

2.1.2. Modifying the OPP problem to keep the observability of the network for all operational topologies

Since the observability is dependent on the topology of the network, the reconfiguration could result in losing the observability. To keep the network observable for all possible topologies, a method is proposed in [6] that is adopted in present section by a revised formulation. This formulation is employed in Appendix A to build a model for the deterministic form of the SOMPP model.

In a reconfigurable network, the buses owning a PMU would remain observable under all topologies, but the observability of the buses with no PMUs, that are observed indirectly by the PMUs of the neighboring buses, might become at risk due to reconfiguration. If all the neighboring buses of these buses are connected to them through a line that is equipped with a tie/sectionalizing switch, they must be observed by all of the neighboring buses. The reason is that the reconfiguration constraints impose the connectivity of all the network buses to it through at least one path, so in any given topology, at least one of the lines connected to these buses would remain in closed state. Consequently, the observability would not be lost if the rest of the connected lines become opened. If the buses without PMUs are connected to one or more lines with fixed state (without any switches), the state of these lines would be kept unchanged due to reconfiguration, so these buses should be observed at least through one of these lines. As a result, the basic OPP problem is altered and the observability coefficients and the desired observability values of the buses would be adjusted by the following procedure:

1. Assume that the network is in its initial configuration. In this situation, for every typical bus i, the degree of bus d_i and the number of tie-switches connected to it $\mathrm{n}_i^{\mathrm{TS}}$ are calculated (The degree of a bus is equal to the number of lines connected to it).
2. The desired observability value for each bus $j \in 1, 2, \ldots, \mathrm{N}$ is calculated as,

$$\mathrm{b}_j^{\mathrm{R}} = \begin{cases} 1 & , \quad \left\{\forall i \in \Lambda_j | \mathrm{a}_{ji} \in \Delta\right\} \\ \mathrm{d}_j + \mathrm{n}_j^{\mathrm{TS}} & , \quad \text{otherwise.} \end{cases} \tag{11}$$

3. The observability coefficients in the case that all the network tie-switches are closed $\mathrm{a}_{ji}^{\mathrm{meshed}}, \forall i, j \in 1, 2, \ldots, \mathrm{N}$ are determined.
4. The observability coefficients to maintain the network observability for all the possible topologies $\mathrm{a}_{ji}^{\mathrm{R}}, \forall i, j \in 1, 2, \ldots, \mathrm{N}$ are specified as follows

$$\mathrm{a}_{ji}^{\mathrm{R}} = \mathrm{a}_{ji}^{\mathrm{meshed}} \times \begin{cases} \mathrm{b}_j^{\mathrm{R}} & , \quad i = j \\ 1 & , \quad \text{otherwise.} \end{cases} \tag{12}$$

The buses without PMUs that are connected to the lines with no switches, should be observed through one of these lines. Therefore, the following constraint should be added to the previous constraints,

$$\mathrm{a}_{jj}^{\mathrm{R}} x_j + \sum_i \mathrm{a}_{ji}^{\mathrm{R}} x_i = 1 \quad , \quad \left\{\forall i \in \Lambda_j | \mathrm{a}_{ji} \in \Delta\right\}. \tag{13}$$

The OPP model considering network reconfiguration could be formulated as,

$$\min \quad \sum_{i=1}^{\mathrm{N}} x_i, \tag{14}$$

$$\text{subject to :} \quad o_j = \sum_{i=1}^{\mathrm{N}} \mathrm{a}_{ji}^{\mathrm{R}} x_i \geq \mathrm{b}_j^{\mathrm{R}}, \quad \forall j \in 1, 2, \ldots, \mathrm{N}. \tag{15}$$

In (14) and (15), the parameters and variables having the superscript R above them are dependent on the problem conditions of this section, while for parameters or variables without a superscript, there is no differences for them between this section and Section 2.1.1.

2.1.3. The effect of channel limit of PMUs on the OPP problem

At the beginning of this section, it is assumed that only the current measurement channels are limited and the formulation of the OPP problem is developed. Then, in the rest of the section, the voltage measurement channel limit is also described briefly in order to extend the proposed model, to include unbalanced distribution networks.

$\forall i \in 1, 2, \ldots, \mathrm{N}$, if $\mathrm{d}_i \leq \mathrm{L}$, the PMU at bus i could measure all the current phasors of adjacent lines of that bus, so the PMU at bus i could be installed only in one way [3,8,19,30]. However, if $\mathrm{d}_i > \mathrm{L}$, the PMU could be installed in $\mathrm{r}_i = \binom{\mathrm{d}_i}{\mathrm{L}}$ different ways [3,8,19,30].

Let $i, j \in 1, 2, \ldots, \mathrm{N}$, $k \in 1, 2, \ldots, \mathrm{r}_i$, and $\Lambda_{ik}^{\mathrm{L}}$ be the kth L-subset of the set of the adjacent buses connected to bus i, Λ_i. Therefore, the observability coefficients are calculated as follows,

$$\mathrm{a}_{ikj}^{\mathrm{CL}} = \begin{cases} 1 & , \quad i = j \text{ or } j \in \Lambda_{ik}^{\mathrm{L}} \\ 0 & , \quad \text{otherwise.} \end{cases} \tag{16}$$

It is worth nothing that if $\forall i \in 1, 2, \ldots, \mathrm{N}$, $\mathrm{d}_i \leq \mathrm{L}$, $\Lambda_{ik}^{\mathrm{L}}$ would be equivalent to Λ_i. The OPP model would be formulated as follows,

$$\min \quad \sum_{i=1}^{\mathrm{N}} \sum_{k=1}^{\mathrm{r}_i} x_{ik}^{\mathrm{CL}}, \tag{17}$$

$$\text{subject to :} \quad o_j = \sum_{i=1}^{\mathrm{N}} \sum_{k=1}^{\mathrm{r}_i} \mathrm{a}_{jik}^{\mathrm{CL}} x_{ik}^{\mathrm{CL}} \geq \mathrm{b}_j, \quad \forall j \in 1, 2, \ldots, \mathrm{N}. \tag{18}$$

In (17) and (18), the parameters and variables with superscript CL are dependent on the conditions of the OPP problem of this section, while the rest of the parameters and variables are just same as those in Section 2.1.1. In order to provide the observability of the network with minimum number of PMUs, $\mathrm{b}_j = 1$, $\forall i \in 1, 2, \ldots, \mathrm{N}$. To calculate $\mathrm{a}_{jik}^{\mathrm{CL}}$, $\mathrm{a}_{ikj}^{\mathrm{CL}}$ is calculated beforehand $\forall i, j \in 1, 2, \ldots, \mathrm{N}$, $k \in 1, 2, \ldots, \mathrm{r}_i$, unlike in Sections 2.1.1 and 2.1.2 that a_{ji} and $\mathrm{a}_{ji}^{\mathrm{R}}$ were calculated directly.

In the case that the voltage measurement channels are not sufficient (e.g. three-phase buses), the number of ways that a PMUs could be installed at a bus should be multiplied by the number of ways that a PMU could measure the voltage phasors. For example, in order to measure the voltage of a three-phase bus, a single-phase PMU could measure the voltage of phases A, B, or C, or it could measure no voltage phasors. Consequently, there are four ways for measuring phase voltage of a three-phase bus by a single-phase PMU. However, the concept could be extended to any arbitrary number of phases and channels. Using this approach, the SOMPP model is extended to include three-phase unbalanced networks. Since the method is beyond the scope of this paper, the details of the formulation are given in Appendix B.

2.1.4. The probability distribution function of uncertain quantities

To compute probabilities of occurrence of the most possible topologies under normal operational condition, the PDF of each uncertain quantity, i.e. power of loads, should be known or calculable. Since the SOMPP problem is a planning problem with a long-term time horizon, the short-term forecasted values of loads powers are not sensible here. As an alternative, seasonal or yearly peak load values become more important. Accordingly, in present paper, the yearly load forecasting values were employed and the optimal configuration would be obtained as a result of reconfiguration operation. If the long-term forecasted peak values were expressed as a set of constant values, the uncertainty of the load forecasting would not be reflected. There are some works in the literature that exploited Gaussian PDF to illustrate the dynamic ranges of forecasted load [34], and a similar procedure is followed in present paper. However, the Gaussian PDF in [34] is employed in transmission level, and in actual distribution networks, the variations of loads do not necessarily follow a known distribution. Nevertheless, it is shown in Section 3.1 that the proposed model could cope with any known or calculable PDFs.

The active and reactive power of loads of a generic bus i are modeled by Gaussian PDFs as follows,

$$\mathrm{pl}_i \sim \mathcal{N}\left(\mu_{\mathrm{pl}_i}, \sigma^2_{\mathrm{pl}_i}\right), \tag{19}$$

$$\mathrm{ql}_i \sim \mathcal{N}\left(\mu_{\mathrm{ql}_i}, \sigma^2_{\mathrm{ql}_i}\right). \tag{20}$$

According to [35], the PDF of failure for a typical line with constant hazard rate during the useful life of the line is represented by an exponential function,

$$f_l = \lambda_l e^{-\lambda_l \tau}. \tag{21}$$

Eq. (21) could represent the PDF of failure for all network lines. The lines that are more likely to be failed would be identified through a MCS procedure that is described in 2.1.5. It is worth mentioning that the lines are considered mission oriented, not repairable from the reliability point of view.

2.1.5. Scenario generation using Monte Carlo simulation method

Scenarios would be generated by random sampling from the PDFs of all existent random variables, i.e. the annual peak of active and reactive power of loads and the TTF of lines. The scenario generating method is taken from [36]. The most frequent technique for producing random samples of a PDF is inverse transform method [36], that is utilized here. Random samples would be the different values of the active and reactive power of loads and the TTF of lines, according to their PDFs. Every scenario is represented by a set of random samples, e.g., the sth scenario is a vector consisting of the sth sampling from all random variables. The probabilities of all generated scenarios would be identical and equal to the reciprocal of the total number of generated scenarios [36].

Each scenario would be composed of one random sample from the PDF of each load and the TTF of each line. According to [35], for a given scenario, if the TTF of a line is greater than or equal to its mission time (e.g. 1 year in present work), the line would be considered in operation, whereas the lines with the TTFs smaller than mission time are considered likely to be failed in the target year.

2.1.6. Scenario reduction approach

Since a great number of scenarios are generated in 2.1.5, there might be lots of scenarios that would be very closed to each other. As a consequence, by applying the scenario reduction methods, the initial set of generated scenarios would be replaced by a few number of representative scenarios. The scenario reduction method that is used in this paper is backward reduction method, that the details could be found in [36]. Using backward reduction method, the initial number of generated scenarios are decreased to a limited number of representative scenarios and the probabilities of the reduced scenarios would be updated meanwhile the scenarios are getting reduced.

2.1.7. Reconfiguration formulation

The reconfiguration would be done for every scenario that is generated by MCS method. Before running the reconfiguration program, active and reactive power of all load points should be set at the sampled values of that scenario. The yielded topologies within each scenario are used in the SOMPP problem.

Reconfiguration is a MINLP problem. Metaheuristic algorithms are widely employed for solving the reconfiguration problem. GA is utilized in present work to find the optimal solution. The most frequent objective of the reconfiguration is minimizing the total active power loss of the network that is one of the objectives of the reconfiguration here. In addition, minimizing the deviation of the voltage magnitude of the buses from the nominal value is also included in the objective function. The formulation of the reconfiguration problem that is given in the following is based on the formulation given in [37].

$$\min \quad \frac{1}{2}\sum_{i=1}^{\mathrm{N}}\sum_{j=1}^{\mathrm{N}}\left[\mathrm{G}_{ij}x_{ij}\left(v_i^2+v_j^2-2v_iv_j\cos\left(\delta_i-\delta_j\right)\right)\right]+\sum_{i=1}^{\mathrm{N}}\left|1-v_i\right|. \tag{22}$$

Subject to:

$$pg_i-\sum_{j=1}^{\mathrm{N}}\left[x_{ij}\left(\mathrm{G}_{ij}v_i^2-v_iv_j\left(\mathrm{G}_{ij}\cos\left(\delta_i-\delta_j\right)+\mathrm{B}_{ij}\sin\left(\delta_i-\delta_j\right)\right)\right)\right]=\mathrm{PL}_i, \tag{23}$$

$$qg_i-\sum_{j=1}^{\mathrm{N}}\left[x_{ij}\left(-\mathrm{B}_{ij}v_i^2-v_iv_j\left(\mathrm{G}_{ij}\sin\left(\delta_i-\delta_j\right)-\mathrm{B}_{ij}\cos\left(\delta_i-\delta_j\right)\right)\right)\right]=\mathrm{QL}_i, \tag{24}$$

$$\frac{1}{2}\sum_{i=1}^{\mathrm{N}}\sum_{j=1}^{\mathrm{N}}x_{ij}=\mathrm{N}-1. \tag{25}$$

There are two types of decision variables in the reconfiguration problem; binary x_{ij} and continuous v_i, δ_i, pg_i and qg_i. If $x_{ij} = 1$, the connecting line between buses i and j would be closed, otherwise, it would be opened. Since $\forall i, j\ x_{ij} = x_{ji}$, the coefficient $\frac{1}{2}$ is used in (22) and (25) before the summations, because each line is considered twice in the formulation. Constraint (25) demonstrates the necessary but not enough condition for radiality of the obtained topology. Radial topology is guaranteed if in addition to satisfying (25), the topology would be connected either. Load flow constraints, (23) and (24), impose the connectivity condition to the problem. It is intended to avoid the complexities associated with the modeling of reconfiguration problem, so some of common constraints, like maximum lines flow restriction, are disregarded deliberately for the sake of simplicity. One could extend the reconfiguration model to include any other purposes.

According to (22)–(25), the number of decision variables are $\mathrm{N}^2+4\mathrm{N}$ that could extremely increase the scale of the optimization problem. However, a large number of variables have known values. If there is no line or tie-switch between buses i and j, then $x_{ij} = x_{ji} = 0$. There is no connection between each bus and itself, so $x_{ii} = 0$. For the buses with no generators $pg_i = 0$ and $qg_i = 0$ and for the slack bus $v_i = 1$ and $\delta_i = 0$.

3. Simulations, numerical results and discussions

The simulation of the proposed model is executed on the benchmark 33-bus distribution network [38] and 240-bus distribution test network [39]. The simulations are conducted by MATLAB R2015b, GAMS 25.1, and OpenDSS 9.4.2.2 softwares on a personal computer with Intel®Core™i7-2670QM 2.20 GHz processor and 8 GB RAM. The ILP model is solved using CPLEX solver in GAMS environment and OpenDSS is used for load flow analysis of the distribution networks.

Table 1
The reduced scenarios introduction for cases I–III (33-bus network).

Case	Scenario no.	Probability	Failed lines	TTF (yr)	Open switches
I	1	0.384	–	–	s9, s14, s28, s32, s33
	2	0.2	–	–	s9, s14, s28, s32, s33
	3	0.416	–	–	s9, s14, s28, s32, s33
II	1	0.39	34	0.0693	s11, s28, s33, s34, s36
			20	0.3083	s11, s13, s17, s20, s28
	2	0.407	13	0.1412	s7, s9, s13, s17, s28
			17	0.2235	s2, s14, s17, s28, s33
			23	0.3166	s7, s9, s14, s23, s32
			20	0.3688	s11, s13, s17, s20, s28
			15	0.5864	s7, s10, s14, s15, s28
			25	0.6712	s9, s14, s25, s32, s33
			34	0.8825	s11, s28, s33, s34, s36
	3	0.203	24	0.4020	s7, s9, s14, s24, s32
			29	0.4937	s2, s14, s17, s28, s33
			35	0.5307	s7, s13, s17, s28, s35
			30	0.5628	s2, s14, s17, s28, s33
			15	0.6660	s7, s10, s14, s15, s28
			33	0.9082	s2, s14, s17, s28, s33
III	1	0.302	35	0.1585	s7, s14, s28, s35, s36
			9	0.2397	s9, s14, s28, s32, s33
			34	0.6651	s2, s13, s28, s33, s34
			2	0.8935	s9, s14, s28, s32, s33
	2	0.227	16	0.1444	s7, s10, s14, s16, s28
			30	0.2037	s9, s14, s28, s30, s33
			32	0.7451	s9, s14, s28, s32, s33
	3	0.471	23	0.1650	s7, s9, s14, s23, s31
			10	0.2714	s10, s14, s28, s32, s33
			8	0.3165	s8, s14, s28, s33, s36
			17	0.5708	s7, s10, s14, s17, s28
			34	0.6850	s11, s28, s32, s33, s34

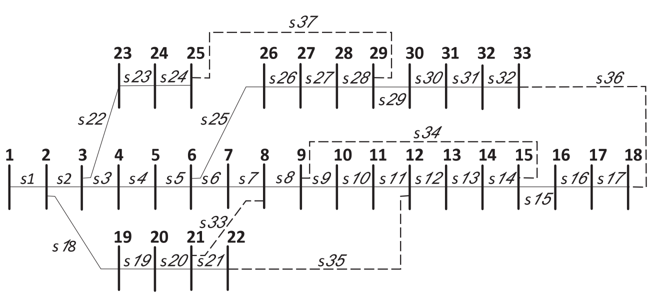

Fig. 4. Benchmark 33-bus distribution network.

3.1. Simulation inputs

In Fig. 4, the one-line diagram of the IEEE 33-bus distribution network is illustrated. Sectionalizing/tie switches are denoted by solid/ dashed lines. It is assumed that all the network lines are equipped with tie switches.

In Fig. 4, the network is in its initial configuration and s33, s34, s35, s36, and s37 are opened. Bus 1 is considered as the slack bus with known magnitude and phase angle ($1\measuredangle 0$ p.u.) and unknown amount of power generation and the rest of the buses are PQ with known power demand and unknown voltage phasor. $\forall i$, The upper and lower bounds of v_i, δ_i, pg_i, and qg_i, are $[0.9, 1.1]$ p.u., $[-\pi/2, \pi/2]$ rad, $[0, 10]$ MW, and $[-10, 10]$ MVAr, respectively. In initial configuration, the total active power loss of the network is 202.7 kW and the sum of the deviations of voltage magnitude of buses is 1.7009 (p.u.). The load demands, given in the 33-bus network data, are considered as the mean values of the Gaussian distributions and coefficient of variations of loads are considered 20%.

The hazard rate of each line according to [40] is considered 0.1 f/yr for the shortest line (100 m) of the network and 0.4 f/yr for the longest one (2000 m). The hazard rates of the rest of the lines take place between aforementioned bounds and increase linearly by increasing the length of lines. The length of lines of 33-bus network are taken from [41].

The GA parameters settings for the reconfiguration problem are as follows: both the population size and the number of iterations are considered 100. The crossover and mutation percent are 80% and 40%, respectively. The mutation rate is assumed 0.4 and the roulette wheel selection method is used for proper selection of parents. The crossover operators are a combination of single-point, double-point and uniform crossover.

The next test network is 240-bus distribution network that is a real network with real smart meter load data. The one-line diagram of the network is shown in Fig. 5. Because the names of the network elements are long and might be confusing, the equivalent numbers are used and the table of equivalent names is given in Appendix C. The network is consisted of three main feeders that the feeders are three, two, and single-phase overhead and underground lines. There are nine circuit breakers in the network that six of them are normally closed and the rest are normally opened. The circuit breakers are specified by small squares in the diagram. The hourly smart meter data of one year (2017) for each load point is available. Since the real load data do not necessarily follow a known PDF, like Gaussian, the PDF of the active and reactive power of loads are estimated using distribution fitting tool in MATLAB. The histogram plot of the active and the reactive power of loads for a given bus (bus 1003) is depicted in Fig. 6 and the estimated PDFs using Gaussian kernels are shown by solid red line. According to Fig. 6, the load data for active power of bus 1003 follows a bimodal distribution and the reactive power follows a non-Gaussian distribution. Since the proposed SOMPP method could be utilized for any random variables with known (or estimated) inverse CDF, the real smart meter data could properly be used in the SOMPP model.

The failure rate of lines are not specified in 240-bus network description, so the failure rate of lines are assumed exactly the same as 33-bus network (0.1 f/yr for 100 m and 0.4 f/yr for 2000 m overhead lines) and the failure rate increases linearly by increasing the length of lines. However, 240-bus network consists of both overhead and underground lines. Since the underground lines are less prone to failure than overheads, after calculating the failure rate of lines, the failure rate of underground lines is assumed to be the half of the calculated values. 240-bus distribution network has a few switches, so, the optimal topologies are obtained using an exhaustive search, by examining all possible combinations of open switches (i.e. three open switches) that result in a radial and connected topology. Moreover, it is assumed that when a line fails, all of its phases would be disconnected from the network. Even though, 240-bus network is unbalanced and solving the SOMPP for a single phase could not be generalized to two other phases, but the proposed SOMPP model is devised for single-phase calculations. Moreover, in order to compare the results of simulations of two test cases, and avoid from complexity, it is assumed that 240-bus network is single-phase and the SOMPP model is solved for a single phase of 240-bus network. The loads that are actually divided among phases are also assumed to be connected to one phase. Same as 33-bus network, bus 1 is considered as the slack bus ($1\measuredangle 0$ p.u.) and all of the load buses are PQ.

3.2. Numerical results and discussions

In this section, the numerical results of simulating the SOMPP model are given and discussed. The simulation results of the deterministic model are also stated in order to compare the results.

3.2.1. Simulation of the SOMPP model

To simulate the SOMPP model, 1000 scenarios are generated. Then, the scenarios are reduced to three representative scenarios. This procedure is performed for four different cases, as following,

Table 2
The reduced scenarios introduction for case IV (240-bus network).

Scenario no.	Probability	Failed lines	TTF (yr)	Open switches/lines
1	0.540	4, 9, 28, 38, 53, 80, 96, 104, 126, 127, 133, 134, 135, 140, 147, 170, 176, 184, 198, 209	0.9158, 0.4822, 0.3903, 0.9324, 0.2283, 0.5670, 0.8387, 0.5039, 0.9871, 0.6343, 0.1485, 0.7852, 0.2833, 0.3708, 0.1107, 0.1676, 0.8936, 0.5937, 0.9544, 0.5237	79, 155, Failed Lines
2	0.175	4, 21, 35, 36, 72, 75, 77, 78, 84, 85, 88, 98, 109, 111, 114, 132, 135, 140, 142, 161, 175, 189	0.9493, 0.6158, 0.5546, 0.7492, 0.5676, 0.5853, 0.2245, 0.2845, 0.4558, 0.8587, 0.9499, 0.1575, 0.0152, 0.8737, 0.4728, 0.5594, 0.3601, 0.0380, 0.7043, 0.1831, 0.9554, 0.5192	44, 79, Failed Lines
3	0.285	9, 14, 18, 22, 75, 83, 105, 108, 146, 147, 154, 195, 212	0.1153, 0.9140, 0.8511, 0.7306, 0.7354, 0.2836, 0.3836, 0.2661, 0.8001, 0.7363, 0.2473, 0.8557, 0.0564	79, 155, Failed Lines

Table 3
The number and the locations of μPMUs for Cases I–III.

Case I			
	Scenario no.	No. of μPMUs	μPMU Buses
L = 1	1	17	1, 3, 4, 7, 9, 11, 14, 16, 18, 19, 20, 22, 24, 26, 27, 30, 32
	2	17	1, 3, 4, 7, 9, 11, 14, 16, 18, 19, 20, 22, 24, 26, 27, 30, 32
	3	17	1, 3, 4, 7, 9, 11, 14, 16, 18, 19, 20, 22, 24, 26, 27, 30, 32
L = 2	1	12	2, 3, 6, 7, 11, 13, 15, 18, 21, 25, 27, 31
	2	12	2, 3, 6, 7, 11, 13, 15, 18, 21, 25, 27, 31
	3	12	2, 3, 6, 7, 11, 13, 15, 18, 21, 25, 27, 31
L = 3	1	12	2, 3, 5, 7, 11, 13, 15, 18, 21, 25, 27, 31
	2	12	2, 3, 5, 7, 11, 13, 15, 18, 21, 25, 27, 31
	3	12	2, 3, 5, 7, 11, 13, 15, 18, 21, 25, 27, 31
Case II			
	Scenario no.	No. of μPMUs	μPMU Buses
L = 1	1	17	1, 3, 4, 6, 8, 9, 12, 14, 15, 18, 19, 21, 23, 25, 27, 30, 33
	2	17	1, 3, 4, 7, 8, 10, 11, 14, 15, 18, 19, 21, 24, 26, 28, 30, 33
	3	17	1, 4, 5, 8, 10, 12, 14, 15, 18, 19, 22, 23, 25, 26, 28, 30, 32
L = 2	1	13	2, 2, 5, 8, 11, 14, 15, 17, 21, 24, 27, 30, 33
	2	13	2, 5, 8, 10, 12, 14, 15, 17, 20, 24, 27, 30, 33
	3	13	2, 4, 8, 10, 12, 14, 16, 21, 24, 26, 29, 32, 33
L = 3	1	16	2, 3, 6, 9, 10, 12, 14, 15, 16, 18, 20, 21, 25, 27, 31, 33
	2	18	2, 3, 6, 8, 9, 10, 11, 12, 14, 15, 17, 18, 20, 21, 25, 27, 31, 33
	3	15	2, 4, 6, 8, 10, 12, 14, 15, 16, 18, 21, 23, 27, 29, 31
Case III			
	Scenario no.	No. of μPMUs	μPMU Buses
L = 1	1	17	1, 3, 4, 6, 8, 9, 11, 12, 14, 16, 19, 22, 24, 27, 29, 31, 33
	2	17	1, 3, 4, 6, 8, 10, 11, 13, 16, 17, 20, 21, 24, 28, 29, 31, 33
	3	18	1, 3, 4, 7, 8, 9, 11, 14, 15, 18, 19, 22, 24, 26, 28, 30, 32, 33
L = 2	1	12	2, 5, 8, 9, 12, 14, 16, 20, 24, 27, 30, 33
	2	12	2, 2, 5, 8, 10, 13, 16, 21, 24, 27, 30, 33
	3	14	2, 5, 8, 10, 11, 14, 15, 17, 21, 23, 27, 29, 31, 33
L = 3	1	15	2, 3, 6, 8, 9, 11, 13, 14, 15, 17, 21, 25, 27, 31, 33
	2	14	2, 3, 6, 8, 10, 12, 14, 15, 18, 20, 23, 27, 29, 31
	3	17	2, 3, 6, 8, 9, 10, 11, 13, 15, 16, 18, 21, 25, 27, 30, 32, 33

I. 33-bus network, considering variability of loads and $L = 1, 2, 3$,

II. 33-bus network considering unreliability of lines and $L = 1, 2, 3$,

III. 33-bus network considering variability of loads, unreliability of lines, and $L = 1, 2, 3$,

IV. 240-bus network considering variability of loads, unreliability of lines, and $L = 1, 2, 3$.

In each case, the probability of each reduced scenario and the optimal topologies within it, are obtained. The term scenario is used instead of reduced scenario henceforward for brevity. The optimal topologies in each scenario are found by reconfiguration. Then, the optimal locations of μPMUs, considering measurement channel limit, are determined, regarding to different number of channels. Due to the paper length limit, the number of channels is considered three at most. The CPU times to generate and reduce the scenarios and finding the optimal topologies are equal to 2771, 9215.1, 7582.2, and 14634.96 s ($\approx$ 4 h) for cases I–IV, respectively.

The generated scenarios for each case are introduced in Tables 1 and 2. Because the number of switching states in case IV is relatively high, the open switches/lines are not given one by one for every topology, and only the name of switches that would be open in each scenario are stated. According to Table 1, in some scenarios, the outage of different lines resulted in an unique topology. However, the repetitive topologies within each scenario are considered once in the SOMPP model. The topology T_0 is also included in all scenarios to be involved in constructing the equivalent network. The open switches in topology

Table 4
The observability of buses with the obtained solution of Case III (L = 3) for all topologies within each scenario.

Open switches	Observability of buses
Scenario 1	
s7, s14, s28, s35, s36	1, 2, 2, 1, 1, 1, 1, 3, 3, 2, 1, 2, 2, 2, 2, 2, 1, 1, 1, 1, 2, 1, 1, 1, 1, 2, 1, 1, 1, 1, 1, 2, 1
s9, s14, s28, s32, s33	1, 2, 2, 1, 1, 1, 2, 2, 3, 1, 1, 2, 2, 2, 2, 2, 1, 2, 1, 1, 1, 1, 1, 1, 1, 2, 1, 1, 1, 1, 1, 1, 1
s2, s13, s28, s33, s34	1, 1, 1, 1, 1, 1, 2, 2, 2, 2, 1, 2, 1, 2, 2, 2, 1, 2, 1, 1, 1, 1, 1, 1, 1, 2, 1, 1, 1, 1, 1, 2, 1
T_0	1, 2, 2, 1, 1, 1, 2, 2, 3, 1, 1, 2, 2, 2, 2, 2, 1, 2, 1, 1, 1, 1, 1, 1, 1, 2, 1, 1, 1, 1, 1, 1, 1
Scenario 2	
s7, s10, s14, s16, s28	1, 2, 3, 1, 1, 1, 1, 1, 3, 1, 1, 1, 2, 1, 1, 1, 1, 1, 2, 1, 2, 1, 2, 1, 1, 2, 1, 1, 1, 2, 1, 1, 1
s9, s14, s28, s30, s33	1, 2, 3, 1, 1, 1, 2, 1, 2, 1, 2, 1, 2, 1, 1, 1, 1, 1, 2, 1, 1, 1, 2, 1, 1, 2, 1, 1, 1, 1, 1, 1, 1
s9, s14, s28, s32, s33	1, 2, 3, 1, 1, 1, 2, 1, 2, 1, 2, 1, 2, 1, 1, 1, 1, 1, 2, 1, 1, 1, 2, 1, 1, 2, 1, 1, 1, 2, 1, 1, 1
T_0	1, 2, 3, 1, 1, 1, 2, 1, 2, 1, 2, 1, 2, 1, 1, 1, 1, 1, 2, 1, 1, 1, 2, 1, 1, 2, 1, 1, 1, 2, 1, 1, 1
Scenario 3	
s7, s9, s14, s23, s31	1, 2, 2, 1, 1, 1, 1, 3, 3, 2, 2, 2, 1, 1, 3, 2, 2, 2, 1, 1, 2, 1, 1, 1, 1, 2, 1, 1, 2, 1, 1, 2, 3
s10, s14, s28, s32, s33	1, 2, 2, 1, 1, 1, 2, 2, 4, 2, 1, 2, 1, 1, 3, 2, 2, 2, 1, 1, 1, 1, 1, 1, 1, 2, 1, 1, 2, 1, 2, 1, 2
s8, s14, s28, s33, s36	1, 2, 2, 1, 1, 1, 2, 1, 3, 3, 2, 2, 1, 1, 3, 2, 2, 1, 1, 1, 1, 1, 1, 1, 1, 2, 1, 1, 2, 1, 2, 2, 2
s7, s10, s14, s17, s28	1, 2, 2, 1, 1, 1, 1, 3, 4, 2, 1, 2, 1, 1, 3, 2, 1, 2, 1, 1, 2, 1, 1, 1, 1, 2, 1, 1, 2, 1, 2, 2, 3
s11, s28, s32, s33, s34	1, 2, 2, 1, 1, 1, 2, 2, 3, 3, 2, 1, 1, 2, 2, 2, 2, 2, 1, 1, 1, 1, 1, 1, 1, 2, 1, 1, 2, 1, 2, 1, 2
T_0	1, 2, 2, 1, 1, 1, 2, 2, 3, 2, 2, 2, 1, 1, 3, 2, 2, 2, 1, 1, 1, 1, 1, 1, 1, 2, 1, 1, 2, 1, 2, 1, 2

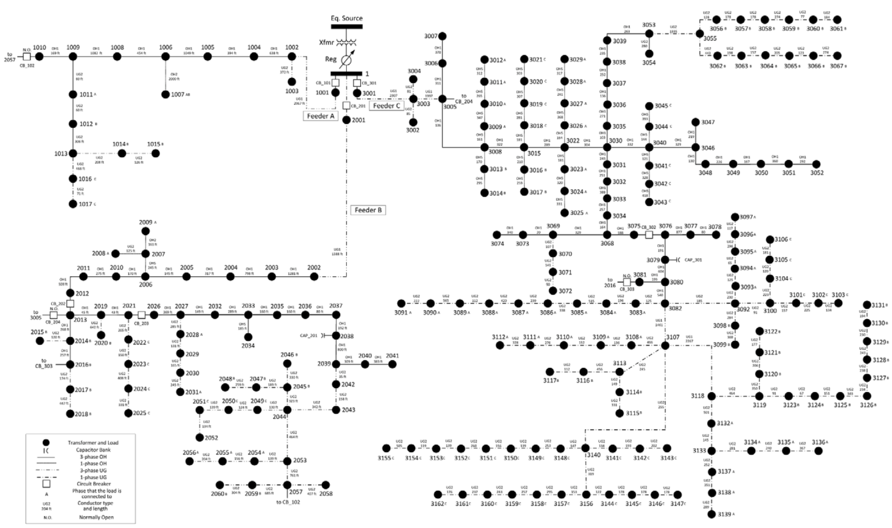

Fig. 5. 240-bus distribution test network [39].

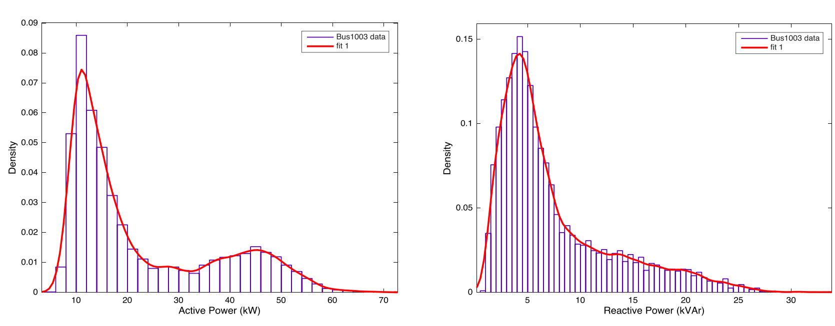

Fig. 6. The histogram plot of the load data for bus 1003 and the fitted PDFs.

T_0 for 33 bus network are s9, s14, s28, s32, and s33, and for 240 bus are 44, 79, and 80.

3.2.1.1. Case I: 33-bus network, considering variability of loads and L = $1, 2, 3$. The simulation results of cases I–III are given in Table 3, and the number of μPMUs and their locations considering different number of channels are stated. In Case I, for a given number of channels, the obtained number of μPMUs for different scenarios are identical, because there is only one optimal topology in each scenario that is identical to the optimal topology of other scenarios and is also equal to T_0, so the SOMPP problem is solved only for one topology. The results of Case I could not be generalized to similar cases, because generally, the load variations could affect on the optimal configuration of the network. Consequently, the variations of loads should not be ignored in the SOMPP Problem. According to Table 3, the number of μPMUs

Table 5
The number and the locations of μPMUs for Case IV.

	Scenario no.	No. of μPMUs	μPMU Buses
L = 1	1	127	1, 1, 4, 6, 8, 10, 10, 12, 13, 16, 17, 20, 21, 24, 25, 26, 28, 31, 33, 34, 35, 38, 39, 40, 42, 46, 48, 50, 51, 53, 56, 57, 59, 62, 63, 66, 67, 69, 72, 73, 75, 77, 80, 81, 83, 84, 86, 87, 90, 92, 94, 97, 98, 100, 103, 104, 107, 109, 112, 113, 115, 117, 119, 120, 123, 124, 126, 127, 129, 132, 133, 135, 137, 139, 141, 142, 145, 146, 147, 150, 152, 153, 156, 157, 160, 163, 165, 167, 168, 171, 172, 175, 177, 178, 178, 181, 183, 185, 185, 188, 190, 193, 195, 198, 199, 201, 203, 204, 207, 209, 210, 211, 211, 214, 216, 218, 221, 222, 225, 226, 228, 231, 233, 234, 235, 237, 239
	2	128	1, 1, 4, 6, 8, 10, 10, 12, 13, 16, 17, 20, 21, 24, 25, 26, 28, 31, 33, 34, 35, 38, 39, 41, 42, 44, 47, 48, 50, 52, 54, 56, 57, 59, 62, 64, 66, 67, 69, 71, 73, 75, 77, 80, 82, 83, 85, 86, 88, 90, 92, 94, 97, 98, 100, 103, 104, 107, 109, 112, 113, 115, 117, 119, 121, 123, 124, 126, 127, 129, 132, 133, 135, 137, 139, 141, 143, 145, 146, 147, 150, 152, 153, 156, 157, 160, 163, 165, 167, 168, 171, 172, 175, 177, 178, 178, 181, 183, 185, 185, 188, 190, 193, 195, 198, 199, 201, 203, 204, 207, 209, 210, 211, 211, 214, 216, 218, 221, 222, 225, 226, 228, 231, 233, 234, 235, 237, 239
	3	127	1, 1, 4, 6, 8, 10, 10, 12, 13, 16, 17, 20, 21, 24, 25, 26, 28, 31, 33, 34, 35, 38, 39, 40, 42, 46, 48, 50, 51, 53, 56, 57, 59, 62, 63, 66, 67, 69, 72, 73, 75, 77, 80, 81, 83, 84, 86, 87, 90, 92, 94, 97, 98, 100, 103, 104, 107, 109, 112, 113, 115, 117, 119, 121, 123, 124, 126, 127, 129, 132, 133, 135, 137, 139, 141, 143, 145, 146, 147, 150, 152, 153, 156, 157, 160, 163, 165, 167, 168, 171, 172, 175, 177, 178, 178, 181, 183, 185, 185, 188, 190, 193, 195, 198, 199, 201, 203, 204, 207, 209, 210, 211, 211, 214, 216, 218, 221, 222, 225, 226, 228, 231, 233, 234, 236, 237, 239
L = 2	1	89	1, 3, 7, 7, 12, 15, 17, 20, 23, 25, 29, 32, 35, 37, 39, 42, 45, 48, 51, 55, 58, 60, 62, 63, 66, 69, 73, 75, 78, 81, 84, 86, 89, 91, 93, 94, 98, 100, 102, 106, 110, 113, 115, 118, 120, 122, 124, 127, 129, 131, 133, 135, 138, 142, 145, 146, 149, 151, 155, 158, 162, 165, 168, 170, 172, 174, 176, 180, 183, 186, 189, 192, 194, 196, 199, 202, 205, 208, 210, 213, 216, 220, 224, 226, 229, 232, 234, 236, 239
	2	88	1, 3, 7, 7, 12, 15, 17, 20, 23, 25, 29, 32, 35, 37, 40, 42, 45, 45, 48, 51, 55, 58, 61, 62, 63, 66, 69, 73, 75, 75, 77, 81, 84, 86, 89, 91, 93, 94, 98, 100, 102, 106, 110, 113, 116, 120, 122, 124, 127, 129, 131, 135, 138, 141, 144, 146, 149, 151, 155, 158, 162, 165, 168, 170, 171, 174, 176, 180, 183, 186, 189, 192, 194, 196, 199, 202, 205, 208, 210, 213, 216, 220, 224, 226, 229, 232, 234, 236, 239
	3	88	1, 3, 7, 7, 12, 15, 17, 20, 23, 25, 29, 32, 35, 37, 39, 42, 45, 48, 51, 55, 58, 60, 62, 63, 66, 69, 73, 75, 77, 81, 84, 86, 89, 91, 93, 94, 98, 100, 102, 106, 110, 112, 113, 116, 120, 122, 124, 127, 129, 131, 135, 138, 141, 144, 149, 151, 153, 155, 158, 162, 165, 168, 170, 172, 174, 176, 180, 183, 186, 189, 192, 194, 196, 199, 202, 205, 208, 210, 213, 216, 220, 224, 226, 229, 232, 234, 236, 239
L = 3	1	88	**3**, 6, **7**, **12**, **15**, **17**, 19, 22, **25**, **29**, **32**, **35**, 38, 39, **42**, **45**, **48**, **51**, 54, 57, **58**, **62**, **63**, **66**, **69**, **73**, **75**, **78**, **81**, **84**, **86**, **89**, **91**, **93**, **94**, **98**, **100**, **102**, **106**, **108**, **110**, **115**, 118, **120**, **122**, **124**, **127**, **129**, **131**, 133, **135**, **138**, 142, 145, **146**, **149**, **151**, **155**, **158**, **162**, **165**, **168**, **170**, **171**, **174**, **176**, **180**, **183**, **186**, **189**, **192**, **194**, **199**, **201**, **202**, **205**, **208**, **210**, **213**, **216**, **220**, **224**, **226**, **229**, **232**, **234**, **236**, **239**
	2	87	**3**, 6, **7**, **12**, **15**, **17**, 19, 22, **25**, **29**, **32**, **35**, 36, **37**, **40**, **42**, **45**, **48**, **51**, 55, **58**, 60, **62**, **63**, **66**, **69**, **73**, **75**, 77, **81**, **84**, **86**, **89**, **91**, **93**, **94**, **98**, **100**, **102**, **106**, **108**, 111, **115**, **120**, **122**, **124**, **127**, **129**, **131**, **135**, **138**, **141**, **144**, **146**, **149**, **151**, **155**, **158**, **162**, **165**, **168**, **170**, **171**, **174**, **176**, **180**, **183**, **186**, **189**, **192**, **194**, **199**, **201**, **202**, **205**, **208**, **210**, **213**, **216**, **220**, **224**, **226**, **229**, **232**, **234**, **236**, **239**
	3	87	**3**, **7**, **12**, **15**, **17**, 20, 23, **25**, **29**, **32**, **35**, **37**, **40**, **42**, **45**, **48**, **51**, 55, 57, **58**, **62**, **63**, **66**, **69**, **73**, **75**, 77, **79**, **81**, **84**, **86**, **89**, **91**, **93**, **94**, **98**, **100**, **102**, **106**, **108**, 111, 112, **115**, **120**, **122**, **124**, **127**, **129**, **131**, **135**, **138**, **141**, **144**, **149**, **151**, 153, 156, **158**, **162**, **165**, **168**, **170**, 172, **174**, **176**, **180**, **183**, **186**, **189**, **192**, **194**, **199**, **201**, **202**, **205**, **208**, **210**, **213**, **216**, **220**, **224**, 227, **229**, **232**, **234**, **236**, **239**

decreases by increasing the number of channels, and the number of μPMUs when L = 2 and L = 3 are identical. Since the cost of μPMUs increases by increasing the number of channels, the μPMUs with 2 channels are preferred in present case.

3.2.1.2. Case II: 33-bus network considering unreliability of lines and L = 1, 2, 3. In this case, it is assumed that the loads would have constant values, while the lines could be failed and their outage could affect on the optimal topology of the network. According to Table 3, the number of μPMUs is relatively more than of Case I, because the diversity of topologies of this case is more than Case I and the number of switches/lines that would be opened/disconnected in the equivalent network of Case II is more than of Case I. The higher number of μPMUs compensates the effect of frequent changes of topology in case II and preserves the observability. By increasing the number of channels from L = 1 to L = 2, the number of μPMUs decreases as expected. But when the number of channels increases to L = 3, the number of μPMUs unexpectedly increases, while the scenarios are kept unchanged and accordingly, the equivalent network for same scenarios would be the same. The authors guess that it might be the best solution that could be found by the solver, because by increasing the number of channels, the scale and the complexity of the problem increases. The locations of μPMUs obtained for different scenarios and a given number of channels are different, but, there are a lot of μPMU buses that are common among different scenarios. The common buses could be good candidates for installing μPMUs.

3.2.1.3. Case III: 33-bus network considering variability of loads, unreliability of lines, and L = 1, 2, 3. In present section, it is assumed that both loads and lines are associated with the degrees of uncertainty. According to Table 3, similar to Case II, the number of μPMUs has been increased compared to Case I, because of the diversity of topologies in all scenarios. However, the number of μPMUs is slightly less than Case II in the same scenarios and the same number of channels, because the diversity of topologies is somewhat less than Case II. The less diversity of topologies is happened because of the variability of loads in Case

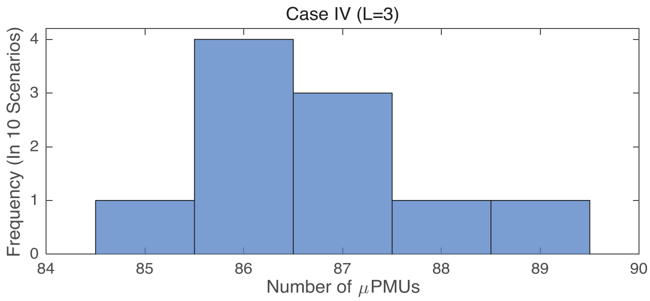

Fig. 7. The histogram plot of the optimal number of μPMUs in 10 scenario — Case IV (L = 3).

III that alleviated the effect of line failures. The number of μPMUs are decreased by increasing the number of channels, but when L = 3, the number of μPMUs unexpectedly increases that might be the best solution that solver could find. The number of common buses among the scenarios are increased compared to Case II, and it reveals that the fewer number of topologies in each scenario leads to the convergence of the outcomes of the scenarios to a similar value.

To verify the equivalent network model, the observability value of buses by the solution obtained in each scenario, for all topologies within it is calculated and listed in Table 4. According to Table 4, the solution that is obtained by the equivalent network of a scenario could provide the observability for all topologies within that scenario. This observability evaluation is also repeated for three other cases and revealed the appropriateness of the equivalent network model.

3.2.1.4. Case IV: 240-bus network considering variability of loads, unreliability of lines, and $L = 1, 2, 3$. In this case, the variability of loads and the probability of line failures are considered simultaneously, similar to Case III, but for 240-bus network, in order to evaluate the SOMPP model for large-scale networks with realistic conditions. The number and the locations of μPMUs are reflected in Table 5 for three scenarios and different number of channels. The simulation results revealed slight difference between the number and the location of μPMUs in three scenarios. However, the number of μPMUs dramatically decreases by increasing the number of channels from L = 1 to L = 2 and L = 3 that justifies using the μPMUs with 2 channels in this Case.

Due to stochastic nature of the problem, three sets of results are obtained from three scenarios. By increasing the number of scenarios, the number of sets of results increases. Actually, representing the stochastic nature of the problem is intended in present work, while, the decision should be made regarding to practical situation requirements. However, in order to demonstrate the consistency of the solution, the simulations of Case IV considering L = 3 are repeated for two different sets of scenarios containing 10 and 50 scenarios that are generated randomly without reducing the scenarios. In Figs. 7 and 8, the frequency of the required number of μPMUs obtained from simulating the sets of scenarios are illustrated by histogram plot. According to Fig. 7, 86 μPMUs is the most frequent value obtained for the random variable of the number of μPMUs. By increasing the number of scenarios in Fig. 8, the mean value of the number of μPMUs approaches to 87. The Figs. 7 and 8 reveal that, if the simulations are repeated a large number of times, the variance of the solution approaches to zero. However, simulating the model for a large number of times is not reasonable, so, the large number of scenarios are reduced and the simulations are run for the reduced scenarios. By comparing Fig. 8 with the results of the simulation of reduced scenarios in Table 5, the effectiveness of reducing the scenarios is revealed.

In addition to the number of μPMUs, the most frequent locations of the μPMUs after simulating 50 scenarios are listed in Table 6. In Table 6, the buses with no μPMUs among 50 scenarios are deleted and only the buses that were the location of μPMUs in more than 70% scenarios are stated with the percentage of the frequency of occurrence. By comparing the Tables 5 and 6, many common buses (that are specified by bold font style in Table 5) are evident and the most frequent μPMU buses that are obtained by simulating a large number of scenarios, are acquired by the reduced scenarios as well.

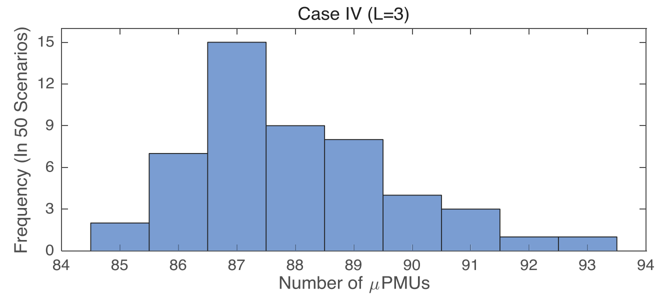

Fig. 8. The histogram plot of the optimal number of μPMUs in 50 scenario — Case IV (L = 3).

Table 6
The buses with more that 70% frequency of occurrence in 50 scenarios — Case IV (L = 3).

Bus	Freq. %	Bus	Freq. %	Bus	Freq. %	Bus	Freq. %
3	98	73	100	127	98	183	100
7	100	75	100	129	98	186	100
12	80	78	98	131	100	189	100
15	82	81	100	135	100	192	100
17	84	84	100	138	100	194	100
25	98	86	98	141	98	199	100
29	92	89	100	144	100	201	98
32	90	91	100	146	92	202	100
35	94	93	98	149	100	205	100
37	94	94	100	151	96	208	100
40	78	98	100	155	96	210	100
42	92	100	96	158	90	213	100
45	96	102	100	162	100	216	100
48	76	106	100	165	100	220	100
51	94	108	100	168	100	224	100
58	90	110	86	170	100	226	94
62	100	115	100	171	90	229	100
63	94	120	100	174	100	232	100
66	98	122	100	176	100	234	100
69	100	124	100	180	100	236	100
						239	100

3.2.2. Compare the SOMPP model with the deterministic model and previous works

In this section, the simulation results of the deterministic version of the SOMPP model (see Appendix A) are given in comparison to the results of simulating the SOMPP model. By this approach, it is assumed that all switches could be open and all lines would be failed in the time horizon of the problem. However, the model is not dependent to the variation of loads. The simulation results are given in Table 7. According to Table 7, the number of μPMUs obtained by the deterministic model is greater than the stochastic one. The numerical results demonstrate the superiority of the stochastic model over the deterministic model in terms of the required number of μPMUs. The difference arises from the fact that the number of topologies that should become observable in the SOMPP model is much less than of the deterministic model.

To compare the proposed model with the previous works, a number of papers from the list of references of this work, that investigated the PMUs/μPMUs placement problem considering reconfiguration and channel limit, in the similar network to present work (33 bus), are selected and the results in terms of the optimal number of PMUs/μPMUs are listed in Table 8. None of the methods listed in Table 8 include a stochastic approach, and the simulation results of the SOMPP model,

Table 7
The number and the locations of μPMUs — deterministic model.

33-Bus network		
Number of channels	Number of μPMUs	μPMUs locations
1	24	2, 3, 5, 6, 8, 9, 11, 12, 13, 14, 15, 17, 18, 19, 21, 22, 23, 25, 26, 28, 29, 31, 32, 33
2	19	2, 3, 5, 7, 8, 9, 11, 13, 15, 17, 20, 21, 22, 24, 26, 28, 29, 31, 33
3	17	2, 3, 5, 6, 8, 10, 12, 13, 15, 17, 20, 21, 24, 27, 29, 31, 33
240-Bus network		
Number of channels	Number of μPMUs	μPMUs locations
1	155	2, 3, 5, 6, 7, 9, 10, 11, 12, 14, 15, 17, 19, 19, 21, 22, 24, 25, 25, 28, 29, 31, , 32, 34, 35, 37, 39, 41, 42, 44, 45, 47, 48, 50, 51, 53, 54, 56, 57, 58, 61, 62, , 63, 65, 68, 69, 71, 72, 73, 75, 77, 79, 81, 81, 83, 84, 86, 88, 89, 91, 93, 94, , 97, 98, 100, 101, 102, 105, 106, 108, 109, 110, 112, 114, 115, 117, 118, , 119, 120, 122, 124, 126, 128, 129, 131, 133, 135, 135, 137, 138, 140, , 141, 143, 144, 146, 147, 148, 149, 151, 154, 155, 157, 158, 160, 162, , 163, 164, 165, 167, 168, 170, 171, 173, 174, 176, 179, 180, 182, 183, , 185, 186, 188, 189, 191, 192, 194, 196, 198, 199, 201, 202, 204, 205, , 207, 208, 210, 212, 213, 215, 216, 218, 219, 220, 223, 224, 227, 228, , 229, 231, 232, 234, 235, 236, 238, 239
2	120	1, 2, 3, 5, 6, 7, 9, 10, 13, 15, 17, 20, 22, 24, 25, 29, 31, 32, 35, 37, 39, 40, , 42, 45, 46, 48, 51, 53, 55, 57, 58, 61, 63, 65, 67, 69, 71, 73, 75, 77, 81, 81, , 83, 84, 87, 89, 91, 93, 94, 96, 98, 100, 102, 104, 106, 108, 110, 112, 114, , 116, 118, 120, 122, 124, 127, 129, 131, 131, 134, 136, 138, 140, 142, , 144, 147, 149, 151, 153, 155, 157, 159, 160, 162, 164, 166, 168, 170, , 172, 174, 176, 178, 180, 183, 185, 187, 189, 192, 194, 196, 197, 199, , 202, 204, 206, 208, 210, 211, 213, 216, 218, 220, 222, 224, 226, 228, , 230, 232, 235, 237, 239
3	115	1, 3, 5, 7, 10, 13, 15, 17, 20, 22, 24, 25, 29, 31, 32, 35, 37, 39, 40, 42, 45, , 46, 48, 51, 54, 56, 57, 58, 61, 63, 65, 67, 69, 71, 73, 75, 77, 81, 84, 86, 86, , 86, 87, 89, 91, 94, 96, 98, 100, 102, 104, 106, 108, 110, 112, 114, 116, , 118, 120, 122, 124, 127, 129, 131, 134, 136, 138, 140, 142, 144, 147, , 149, 151, 153, 155, 157, 159, 160, 162, 164, 166, 168, 170, 172, 174, , 176, 178, 180, 183, 185, 187, 189, 192, 194, 196, 197, 199, 202, 204, , 206, 208, 211, 213, 216, 218, 220, 222, 224, 226, 228, 230, 232, 235, , 237, 239

Table 8
Comparing the SOMPP model with the previous works.

Proposed method	No. of PMUs/μPMUs	Reconfiguration	Channel limit
SOMPP	17–18	Yes	Yes (L = 1)
	12–14	Yes	Yes (L = 2)
	14–17	Yes	Yes (L = 3)
[25]	12	Yes (2 topologies)	No
	12	No	Yes (L = 2)
	13	Yes (6 topologies)	No
	13	Yes (6 topologies)	Yes (L = 2)
[6]	17	Yes (all topologies)	No
[23]	14–22	Yes	No
[22]	14–22	Yes	No

only for Case III are reflected. According to Table 8, the SOMPP model could be compared with the method of [25] when L = 2 and 6 topologies are considered. The 6 topologies are predefined and cover all operational topologies of the network. The SOMPP model has shown a slight superiority to the method of [25] in some scenarios, while the solutions are obtained by a stochastic approach considering the operational topologies and line failures. The proposed method obtained a better solution in terms of the number of required μPMUs compared to [6], because the topologies with less probability of occurrence are not included in the model.

Comparing the results of the SOMPP model with the results of the deterministic version and previous works reveals the relative superiority of the SOMPP model in decreasing the required number of μPMUs. However, the authors are aware of the drawbacks of the model. One of the main drawbacks of the method is that the proposed model does not include a decision making procedure to identify the best solution among the set of scenarios. Another drawback of the method is that it only considers the most probable topologies, and if a rare configuration happens, the observability of the network will not be guaranteed.

4. Conclusion

An ILP model for stochastic optimal placement of μPMUs considering the risk of losing observability following a reconfiguration operation is investigated in present paper. The channel limit for voltage measurements is also introduced in addition to considering the current channels limit, in order to increase the flexibility of the model to be extended to the cases that voltage channels are not sufficient for full observability of a single bus (e.g. three-phase networks). To prevent unobservability of the network due to reconfiguration, a stochastic approach is addressed in which the most important topologies are incorporated in the ILP model, rather than considering all of them. The uncertain variables included in the model are the active and reactive power of loads and the TTF of lines that are described by proper PDFs instead of fixed probability values. The PDFs of the uncertain variables are utilized in a MCS and a number of probable scenarios for loads and failed lines are generated. Then the network is reconfigured for each scenario and a number of topologies are obtained within each scenario that are most likely to be happened. The SOMPP model is solved using these scenarios and the concept of equivalent network that is introduced in present work. The deterministic version of the proposed model, that considers the observability of the network for all possible topologies with limited number of channels is developed in order to be compared with the stochastic method. The formulation of the SOMPP model is also extended using the concept of voltage channel limit in order to include the unbalanced networks.

The simulations are executed considering the uncertainty of loads and the unreliability of lines separately and simultaneously. The superiority of the model in minimizing the number of μPMUs is revealed by comparing the simulation results with the deterministic model and previous works. The success of the model in handling the random variables with unknown PDFs is demonstrated by using the real smart meter data. The effectiveness of the reduced scenarios in representing the most general scenarios is also determined by simulating the model for a large number of scenarios. It is also concluded that the concept of equivalent network could properly provide the observability for all topologies of each scenario.

In future studies, more smart grid elements with stochastic nature, such as distributed generators based on renewable energy resources, electric vehicles, demand response, etc. could be incorporated. The SOMPP model for unbalanced networks could also be formulated with more details to reflect the realistic aspects of the distribution networks.

CRediT authorship contribution statement

Nasim Khanjani: Conceptualization, Methodology, Software, Writing – original draft. **Seyed Masoud Moghaddas-Tafreshi:** Supervision, Conceptualization, Writing – review & editing.

Declaration of competing interest

The authors declare that they have no known competing financial interests or personal relationships that could have appeared to influence the work reported in this paper.

Data availability

Data will be made available on request.

Appendix A. The formulation of the deterministic model

The deterministic version of the proposed SOMPP problem considering both reconfiguration and μPMUs channel limit is developed to compare the results of the stochastic and the deterministic models. The difference between the deterministic and the stochastic models is that in the deterministic model, all the possible topologies are included, while, in the stochastic approach, only the most probable topologies are considered.

The optimization model is given in (A.1) and (A.2),

$$\min \quad \sum_{i=1}^{N}\sum_{k=1}^{r_i} x_{ik}^{RCL}, \tag{A.1}$$

$$\text{subject to}: \quad o_j = \sum_{i=1}^{N}\sum_{k=1}^{r_i} a_{jik}^{RCL} x_{ik}^{RCL} \geq b_j^{RCL} \quad , \quad \forall j \in 1,2,\ldots,N. \tag{A.2}$$

The parameters and variables with superscript RCL are affected by the condition of the deterministic model. The desired observability values b_j^{RCL} are calculated similar to (11), and the method of determining the observability coefficients a_{jik}^{RCL} is analogous to that of a_{ikj}^{CL} in (16). However, there are some points that should be taken into the consideration in the deterministic model:

- All the network tie-switches must be in closed state and therefore the network should have a meshed configuration.
- For a typical bus i, if $d_i + n_i^{TS} \leq L$, the μPMU would be installed on bus i in a unique manner, but, if $d_i + n_i^{TS} > L$, the μPMU at bus i could be installed in $r_i = \binom{d_i + n_i^{TS}}{L}$ different ways.

Appendix B. The SOMPP formulation for unbalanced networks

The proposed SOMPP model is devised for three-phase balanced networks and is solved for one of the phases, while the result could be generalized to other phases. Since the actual distribution networks are mostly unbalanced with three, two, and single-phase feeders, the proposed SOMPP model could be extended to include the unbalanced networks. The method is briefly described in the following, but the simulation results are disregarded due to length limit of the paper.

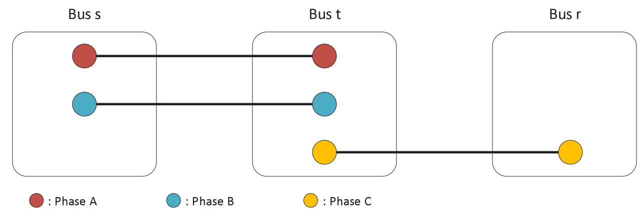

Fig. B.9. An example of an unbalanced network.

The formulation is based on an assumption; the μPMUs are considered single-phase with one voltage and L current measurement channels. Accordingly, for the example network of Fig. B.9, a μPMU could measure the voltage of bus t in three and the current of the lines connected to the phases of bus t in $\binom{3}{L}$ different ways. Consequently, the total number of ways that a μPMU could be installed at bus t is $3 \times \binom{3}{L}$. On the other hand, for bus r, there is only one way that a μPMU could be installed at this bus, because there is only one voltage and one current phasor that should be measured. This procedure could be employed to establish a framework for the SOMPP model of the unbalanced network.

The formulation of the SOMPP model for an unbalanced network could be expressed as,

$$\min: \quad p_s \sum_{i=1}^{N} \sum_{h\in\{A,B,C\}} \sum_{k=1}^{r_{sih}^{EQ}} x_{sihk}^{EQ}, \tag{B.1}$$

$$\text{subject to}: \quad o_{sjg} = \sum_{i=1}^{N} \sum_{h\in\{A,B,C\}} \sum_{k=1}^{r_{sih}^{EQ}} a_{sjgihk}^{EQ} x_{sihk}^{EQ} \geq b_{sjg}, \tag{B.2}$$

$$s \in 1,2,\ldots,S', \quad \forall j \in 1,2,\ldots,N, \quad g \in \{A,B,C\}.$$

According to (B.1), A, B, and C represent the three phases. In order to calculate r_{sih}^{EQ}, the parameter d_i^{3PH} is introduced that is called the three-phase degree of bus i, and is equal to the number of phases connected to bus i from adjacent buses. For example in Fig. B.9, $d_t^{3PH} = 3$. Now, if $d_i^{3PH} \leq L$, the μPMU could be install at bus i only in a single way and $r_{sih}^{EQ} = 1$, while if $d_i^{3PH} > L$, the μPMU could be installed in $r_{sih}^{EQ} = \binom{d_i^{3PH}}{L}$ different ways.

The observability of the network is determined by the observability of all phases at each bus. In (B.2), a_{sihkjg}^{EQ} is determined by the following equation,

$$a_{sihkjg}^{EQ} = \begin{cases} 1 & , \quad (i,h) = (j,g) \text{ OR } (j,g) \in \Lambda_{ik}^{L3PH} \\ 0 & , \quad \text{otherwise.} \end{cases} \tag{B.3}$$

In (B.3), $\left\{\forall i \in 1,2,\ldots,N | d_i^{3PH} \leq L\right\}$, the kth L-subset of the set of adjacent bus phases of bus i, i.e. Λ_{ik}^{L3PH}, is equal to the set of adjacent bus phases of bus i, i.e. Λ_i^{3PH}. The elements of Λ_i^{3PH} are the ordered pairs, like (i,h). For example, in Fig. B.9, $\Lambda_t^{3PH} = \{(s,A),(s,B),(\mathbf{r},\mathbf{C})\}$. The values of b_{sjg} are considered equal to one in order to minimize the number of μPMUs required for the observability of the network.

Appendix C. The table of 240-bus network equivalent names for buses and lines

See Table C.9.

Table C.9
The equivalent names for buses and lines of 240-bus network.

F.	T.	F. Eq.	T. Eq.	L. Eq.	F.	T.	F. Eq.	T. Eq.	L. Eq.
1	1001	1	2	1	3060	3061	138	139	123
1001	1002	2	3	2	3055	3062	133	140	124
1002	1003	3	4	3	3062	3063	140	141	125
1002	1004	3	5	4	3063	3064	141	142	126
1004	1005	5	6	5	3064	3065	142	143	127
1005	1006	6	7	6	3065	3066	143	144	128
1006	1007	7	8	7	3066	3067	144	145	129
1006	1008	7	9	8	3030	3040	108	118	130
1008	1009	9	10	9	3040	3044	118	122	131
1009	1010	10	11	10	3044	3045	122	123	132
1009	1011	10	12	11	3040	3041	118	119	133
1011	1012	12	13	12	3041	3042	119	120	134
1012	1013	13	14	13	3042	3043	120	121	135
1013	1014	14	15	14	3040	3046	118	124	136
1014	1015	15	16	15	3046	3047	124	125	137
1013	1016	14	17	16	3046	3048	124	126	138
1016	1017	17	18	17	3048	3049	126	127	139
1010	2057	11	75	18	3049	3050	127	128	140
1	2001	1	19	19	3050	3051	128	129	141
2001	2002	19	20	20	3051	3052	129	130	142
2002	2003	20	21	21	3030	3031	108	109	143
2003	2004	21	22	22	3031	3032	109	110	144
2004	2005	22	23	23	3032	3033	110	111	145
2005	2006	23	24	24	3033	3034	111	112	146
2006	2007	24	25	25	3034	3068	112	146	147
2007	2008	25	26	26	3068	3069	146	147	148
2007	2009	25	27	27	3069	3070	147	148	149
2006	2010	24	28	28	3070	3071	148	149	150
2010	2011	28	29	29	3071	3072	149	150	151
2011	2012	29	30	30	3069	3073	147	151	152
2012	2013	30	31	31	3073	3074	151	152	153
2013	2014	31	32	32	3068	3075	146	153	154
2014	2015	32	33	33	3075	3076	153	154	155
2014	2016	32	34	34	3076	3077	154	155	156
2016	2017	34	35	35	3077	3078	155	156	157
2017	2018	35	36	36	3076	3079	154	157	158
2013	2019	31	37	37	3079	3080	157	158	159
2019	2020	37	38	38	3080	3081	158	159	160
2019	2021	37	39	39	3080	3082	158	160	161
2021	2022	39	40	40	3081	2016	159	34	162
2022	2023	40	41	41	3082	3083	160	161	163
2023	2024	41	42	42	3083	3084	161	162	164
2024	2025	42	43	43	3084	3085	162	163	165
2021	2026	39	44	44	3085	3086	163	164	166
2026	2027	44	45	45	3086	3087	164	165	167
2027	2028	45	46	46	3087	3088	165	166	168
2028	2029	46	47	47	3088	3089	166	167	169
2029	2030	47	48	48	3089	3090	167	168	170
2030	2031	48	49	49	3090	3091	168	169	171
2027	2032	45	50	50	3082	3092	160	170	172
2032	2033	50	51	51	3092	3093	170	171	173
2033	2034	51	52	52	3093	3094	171	172	174
2033	2035	51	53	53	3094	3095	172	173	175
2035	2036	53	54	54	3095	3096	173	174	176
2036	2037	54	55	55	3096	3097	174	175	177
2037	2038	55	56	56	3092	3098	170	176	178
2038	2039	56	57	57	3098	3099	176	177	179
2039	2040	57	58	58	3092	3100	170	178	180
2040	2041	58	59	59	3100	3101	178	179	181
2039	2042	57	60	60	3101	3102	179	180	182
2042	2043	60	61	61	3102	3103	180	181	183
2043	2044	61	62	62	3100	3104	178	182	184
2044	2045	62	63	63	3104	3105	182	183	185
2045	2046	63	64	64	3105	3106	183	184	186
2045	2047	63	65	65	3082	3107	160	185	187
2047	2048	65	66	66	3107	3108	185	186	188
2044	2049	62	67	67	3108	3109	186	187	189
2049	2050	67	68	68	3109	3110	187	188	190
2050	2051	68	69	69	3110	3111	188	189	191
2051	2052	69	70	70	3111	3112	189	190	192
2044	2053	62	71	71	3107	3113	185	191	193

Table C.9 (*continued*).

F.	T.	F. Eq.	T. Eq.	L. Eq.	F.	T.	F. Eq.	T. Eq.	L. Eq.
2053	2054	71	72	72	3113	3114	191	192	194
2054	2055	72	73	73	3114	3115	192	193	195
2055	2056	73	74	74	3113	3116	191	194	196
2053	2057	71	75	75	3116	3117	194	195	197
2057	2058	75	76	76	3107	3118	185	196	198
2057	2059	75	77	77	3118	3119	196	197	199
2059	2060	77	78	78	3119	3120	197	198	200
2013	3005	31	83	79	3120	3121	198	199	201
1	3001	1	79	80	3121	3122	199	200	202
3001	3003	79	81	81	3119	3123	197	201	203
3003	3002	81	80	82	3123	3124	201	202	204
3003	3004	81	82	83	3124	3125	202	203	205
3003	3005	81	83	84	3125	3126	203	204	206
3005	3006	83	84	85	3126	3127	204	205	207
3006	3007	84	85	86	3127	3128	205	206	208
3005	3008	83	86	87	3128	3129	206	207	209
3008	3009	86	87	88	3129	3130	207	208	210
3009	3010	87	88	89	3130	3131	208	209	211
3010	3011	88	89	90	3118	3132	196	210	212
3011	3012	89	90	91	3132	3133	210	211	213
3008	3013	86	91	92	3133	3134	211	212	214
3013	3014	91	92	93	3134	3135	212	213	215
3008	3015	86	93	94	3135	3136	213	214	216
3015	3016	93	94	95	3133	3137	211	215	217
3016	3017	94	95	96	3137	3138	215	216	218
3015	3018	93	96	97	3138	3139	216	217	219
3018	3019	96	97	98	3107	3140	185	218	220
3019	3020	97	98	99	3140	3141	218	219	221
3020	3021	98	99	100	3141	3142	219	220	222
3015	3022	93	100	101	3142	3143	220	221	223
3022	3023	100	101	102	3140	3148	218	226	224
3023	3024	101	102	103	3148	3149	226	227	225
3024	3025	102	103	104	3149	3150	227	228	226
3022	3026	100	104	105	3150	3151	228	229	227
3026	3027	104	105	106	3151	3152	229	230	228
3027	3028	105	106	107	3152	3153	230	231	229
3028	3029	106	107	108	3153	3154	231	232	230
3022	3030	100	108	109	3154	3155	232	233	231
3030	3035	108	113	110	3140	3156	218	234	232
3035	3036	113	114	111	3156	3144	234	222	233
3036	3037	114	115	112	3144	3145	222	223	234
3037	3038	115	116	113	3145	3146	223	224	235
3038	3039	116	117	114	3146	3147	224	225	236
3039	3053	117	131	115	3156	3157	234	235	237
3053	3054	131	132	116	3157	3158	235	236	238
3053	3055	131	133	117	3158	3159	236	237	239
3055	3056	133	134	118	3159	3160	237	238	240
3056	3057	134	135	119	3160	3161	238	239	241
3057	3058	135	136	120	3161	3162	239	240	242
3058	3059	136	137	121					
3059	3060	137	138	122					

References

[1] Ahmadi A, Alinejad-Beromi Y, Moradi M. Optimal PMU placement for power system observability using binary particle swarm optimization and considering measurement redundancy. Expert Syst Appl 2011;38(6):7263–9.

[2] Zhao Y, Yuan P, Ai Q, Lv T. Optimal PMU placement considering topology constraints. Int J Electr Power Energy Syst 2015;73:240–8.

[3] Abiri E, Rashidi F, Niknam T, Salehi MR. Optimal PMU placement method for complete topological observability of power system under various contingencies. Int J Electr Power Energy Syst 2014;61:585–93.

[4] Azizi S, Salehi-Dobakhshari A, Nezam-Sarmadi SA, Ranjbar AM. Optimal PMU placement by an equivalent linear formulation for exhaustive search. IEEE Trans Smart Grid 2012;3(1):174–82.

[5] Bečejac V, Stefanov P. Groebner bases algorithm for optimal PMU placement. Int J Electr Power Energy Syst 2020;115:105427.

[6] Su H, Wang C, Li P, Liu Z, Yu L, Wu J. Optimal placement of phasor measurement unit in distribution networks considering the changes in topology. Appl Energy 2019;250:313–22.

[7] Mohamed MA, Al-Sumaiti AS, Krid M, Awwad EM, Kavousi-Fard A. A reliability-oriented fuzzy stochastic framework in automated distribution grids to allocate μ-PMUs. IEEE Access 2019;7:33393–404.

[8] Shafiullah M, Hossain MI, Abido M, Abdel-Fattah T, Mantawy A. A modified optimal PMU placement problem formulation considering channel limits under various contingencies. Measurement 2019;135:875–85.

[9] Huang Y, Li S, Liu X, Zhang Y, Sun L, Yang K. A probabilistic multi-objective model for phasor measurement units placement in the presence of line outage. Sustainability 2019;11(24):7097.
[10] Gomez O, Rios MA, Anders G. Reliability-based phasor measurement unit placement in power systems considering transmission line outages and channel limits. IET Gener Transm Distrib 2014;8(1):121–30.
[11] Ghamsari-Yazdel M, Esmaili M. Reliability-based probabilistic optimal joint placement of PMUs and flow measurements. Int J Electr Power Energy Syst 2016;78:857–63.
[12] Babu R, Bhattacharyya B. Strategic placements of PMUs for power network observability considering redundancy measurement. Measurement 2019;134:606–23.
[13] Devi MM, Geethanjali M. Hybrid of genetic algorithm and minimum spanning tree method for optimal PMU placements. Measurement 2020;154:107476.
[14] Aminifar F, Fotuhi-Firuzabad M, Shahidehpour M, Khodaei A. Probabilistic multistage PMU placement in electric power systems. IEEE Trans Power Deliv 2010;26(2):841–9.
[15] Razavi S-E, Falaghi H, Nezhad AE, Moghaddam MJH, Gandoman FH. An effective approach for the probabilistic and deterministic multistage PMU placement using cuckoo search: Iran's national power system. Iran J Sci Technol Trans Eng 2020;44(1):237–52.
[16] Aghaei J, Baharvandi A, Rabiee A, Akbari M-A. Probabilistic PMU placement in electric power networks: an MILP-based multiobjective model. IEEE Trans Ind Inf 2015;11(2):332–41.
[17] Guo X-C, Liao C-S, Chu C-C. Probabilistic optimal PMU placements under limited observability propagations. IEEE Syst J 2021.
[18] Wang S, Huang R, Ke X, Zhao J, Fan R, Wang H, et al. Risk-oriented PMU placement approach in electric power systems. IET Gener Transm Distrib 2020;14(2).
[19] Okekunle DJ, Unigwe O, Kiprakis AE. Optimal co-placement method considering non-homogeneous PMU channel capacities. IET Smart Grid 2020;3(5):626–37.
[20] Chen X, Wei F, Cao S, Soh CB, Tseng KJ. PMU placement for measurement redundancy distribution considering zero injection bus and contingencies. IEEE Syst J 2020;14(4):5396–406.
[21] Koochi MHR, Hemmatpour MH. A general PMU placement approach considering both topology and system aspects of contingencies. Int J Electr Power Energy Syst 2020;118:105774.
[22] Abdelsalam HA, Abdelaziz AY, Mukherjee V. Optimal PMU placement in a distribution network considering network reconfiguration. In: 2014 International conference on circuits, power and computing technologies. IEEE; 2014, p. 191–6.
[23] Abdelsalam HA, Abdelaziz AY, Osama RA, Salem RH. Impact of distribution system reconfiguration on optimal placement of phasor measurement units. In: 2014 Clemson university power systems conference. IEEE; 2014, p. 1–6.
[24] Chauhan K, Sodhi R. Placement of distribution-level phasor measurements for topological observability and monitoring of active distribution networks. IEEE Trans Instrum Meas 2019;1.
[25] Dua GS, Tyagi B, Kumar V. Deploying micro-PMUs with channel limit in reconfigurable distribution systems. IEEE Syst J 2021.
[26] Moradi-Sepahvand M, Mashhour E, Mortazavi SS. Optimal placement of a combination of single-phase and three-phase μPMUs for observability of smart distribution networks with asymmetrical structure. Int J Electr Power Energy Syst 2019;105:592–601.
[27] Elsayed AAE, Mohamed MA, Abdelraheem M, Nayel MA. Optimal μPMU placement based on hybrid current channels selection for distribution grids. IEEE Trans Ind Appl 2020;56(6):6871–81.
[28] Biswas RS, Azimian B, Pal A. A micro-PMU placement scheme for distribution systems considering practical constraints. In: 2020 IEEE power & energy society general meeting. IEEE; 2020, p. 1–5.
[29] Anguswamy MP, Datta M, Meegahapola L, Vahidnia A. Optimal micro-PMU placement in distribution networks considering usable zero-injection phase strings. IEEE Trans Smart Grid 2022.
[30] Elaziez AA, Mohamed MA, AbdelRaheem M, Nayel MA. Optimal μPMU placement and current channel selection considering running cost for distribution grid. In: 2020 IEEE international conference on power electronics, smart grid and renewable energy. IEEE; 2020, p. 1–8.
[31] Dutta S, Sadhu PK, Reddy MJB, Mohanta DK. Role of microphasor measurement unit for decision making based on enhanced situational awareness of a modern distribution system. In: Decision making applications in modern power systems. Elsevier; 2020, p. 181–99.
[32] Khanjani N, Moghaddas-Tafreshi SM. Analysis of observability constraint on optimal feeder reconfiguration of an active distribution network with μPMUs. In: 2020 28th Iranian conference on electrical engineering. IEEE; 2020, p. 1–5.
[33] Borozan V, Rajicic D, Ackovski R. Minimum loss reconfiguration of unbalanced distribution networks. IEEE Trans Power Deliv 1997;12(1):435–42.
[34] Dalvand MM, Azami SBZ, Tarimoradi H. Long-term load forecasting of Iranian power grid using fuzzy and artificial neural networks. In: 2008 43rd international universities power engineering conference. IEEE; 2008, p. 1–4.
[35] Billinton R, Allan RN. Reliability evaluation of engineering systems. Springer; 1992.
[36] Siahkali H, Vakilian M. Stochastic unit commitment of wind farms integrated in power system. Electr Power Syst Res 2010;80(9):1006–17.
[37] Lavorato M, Franco JF, Rider MJ, Romero R. Imposing radiality constraints in distribution system optimization problems. IEEE Trans Power Syst 2011;27(1):172–80.
[38] Baran ME, Wu FF. Network reconfiguration in distribution systems for loss reduction and load balancing. IEEE Trans Power Deliv 1989;4(2):1401–7.
[39] Bu F, Yuan Y, Wang Z, Dehghanpour K, Kimber A. A time-series distribution test system based on real utility data. In: 2019 North American power symposium. IEEE; 2019, p. 1–6.
[40] Sedighizadeh M, Esmaili M, Mahmoodi M. Reconfiguration of distribution systems to improve reliability and reduce power losses using imperialist competitive algorithm. Iran J Electr Electron Eng 2017;13(3):287–302.
[41] Ghasemi S, Moshtagh J. Radial distribution systems reconfiguration considering power losses cost and damage cost due to power supply interruption of consumers. Int J Electr Eng Inform 2013;5(3).